



**Volodymyr Magas**

*University of Barcelona, Spain*

**Tilted initial state:**

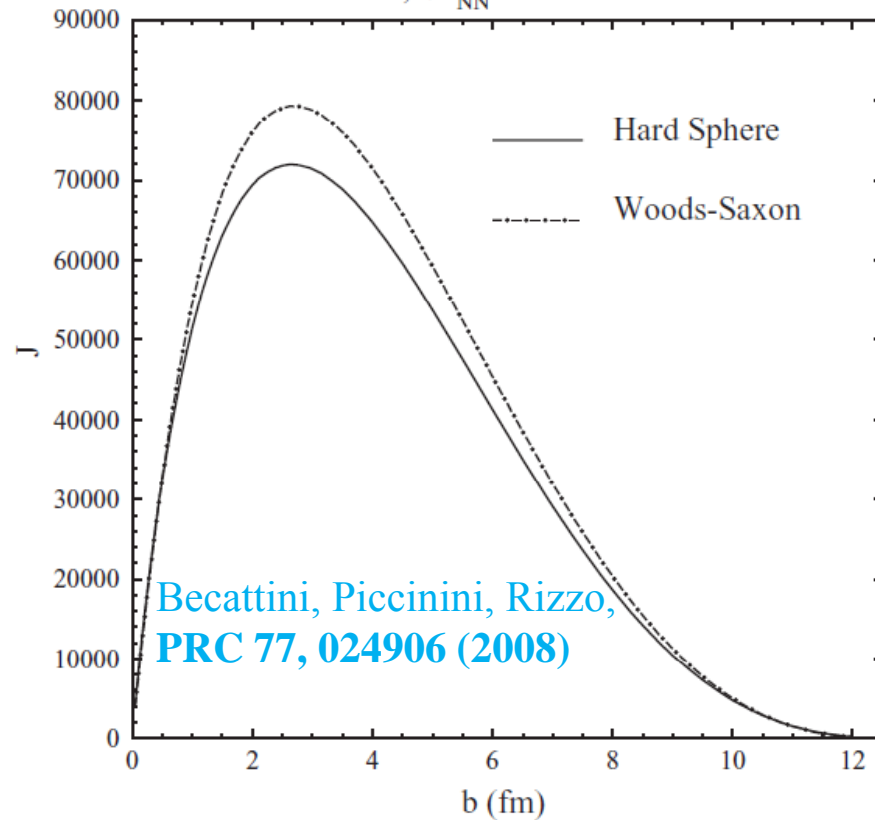
**reasons and consequence**

**Nuclei colliding at ultra-relativistic energies  
with nonzero impact parameter  
have a large initial angular momentum,**

**which is usually ignored  
in the initial conditions assumed for hydro calculations**

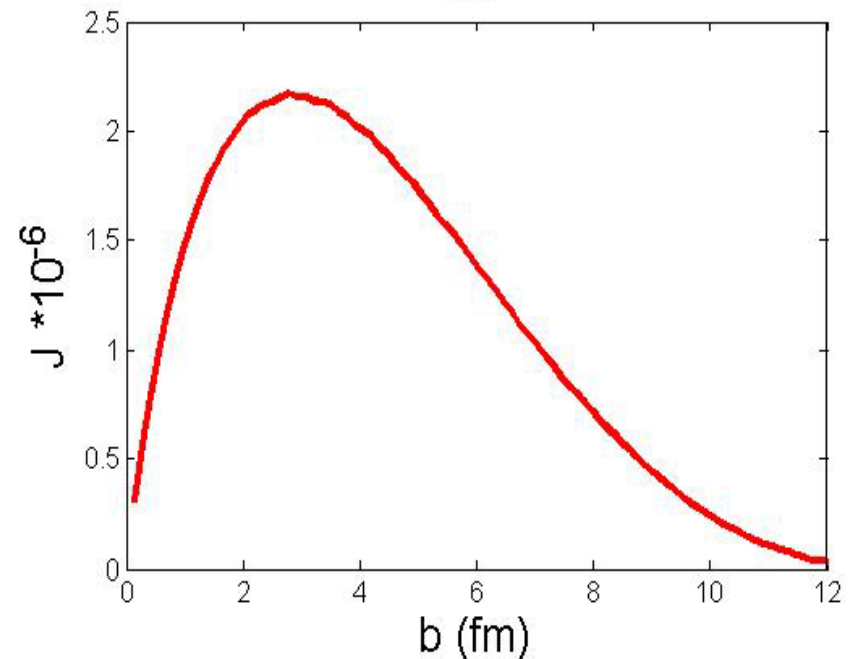
**RHIC:  $J \simeq 5 \cdot 10^4$**

Au Au,  $\sqrt{s_{NN}} = 200$  GeV

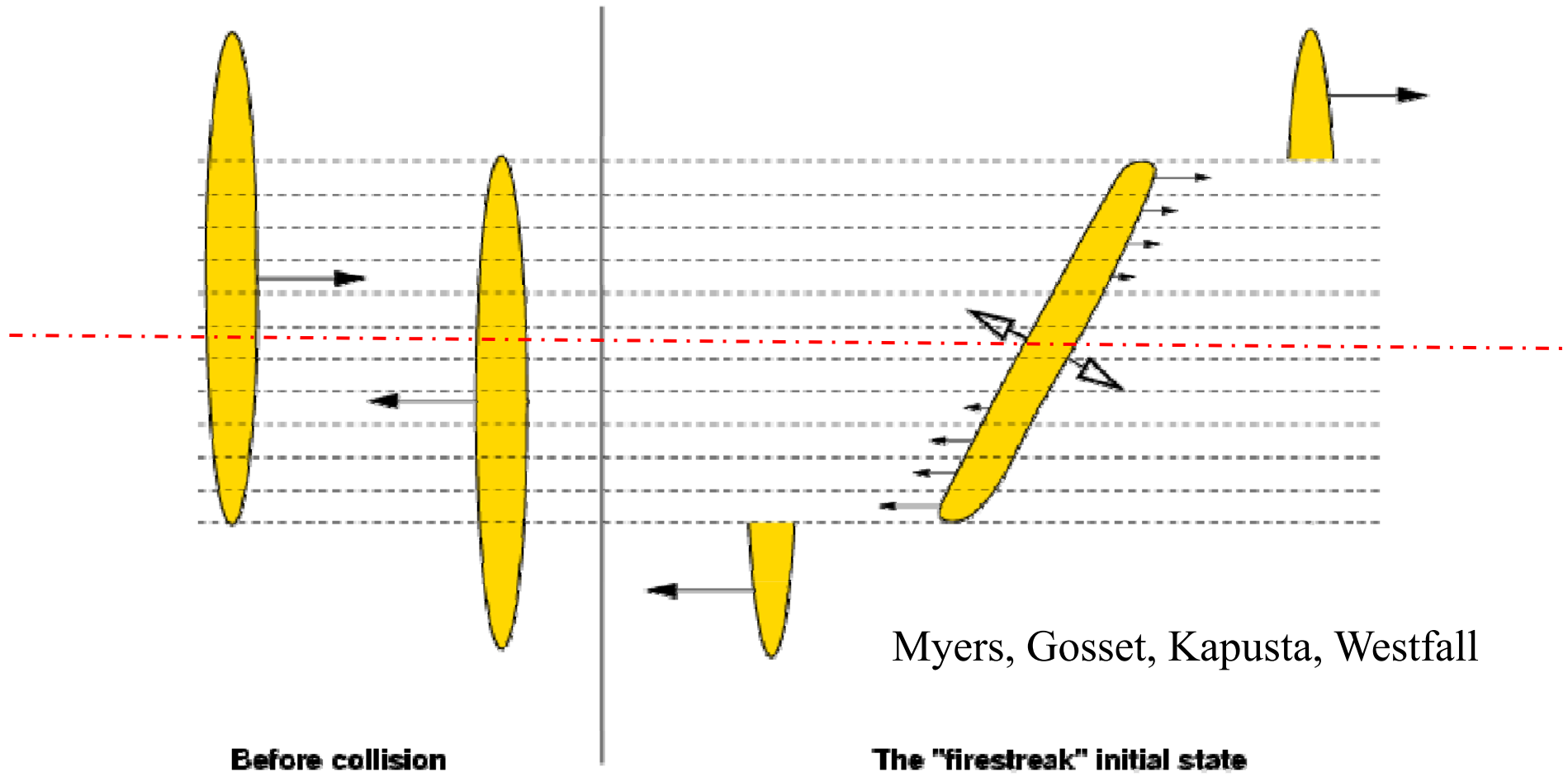


**LHC:  $J \simeq 1.5 \cdot 10^6$**

Pb+Pb,  $s_{NN}^{-1/2} = 5.5$  TeV



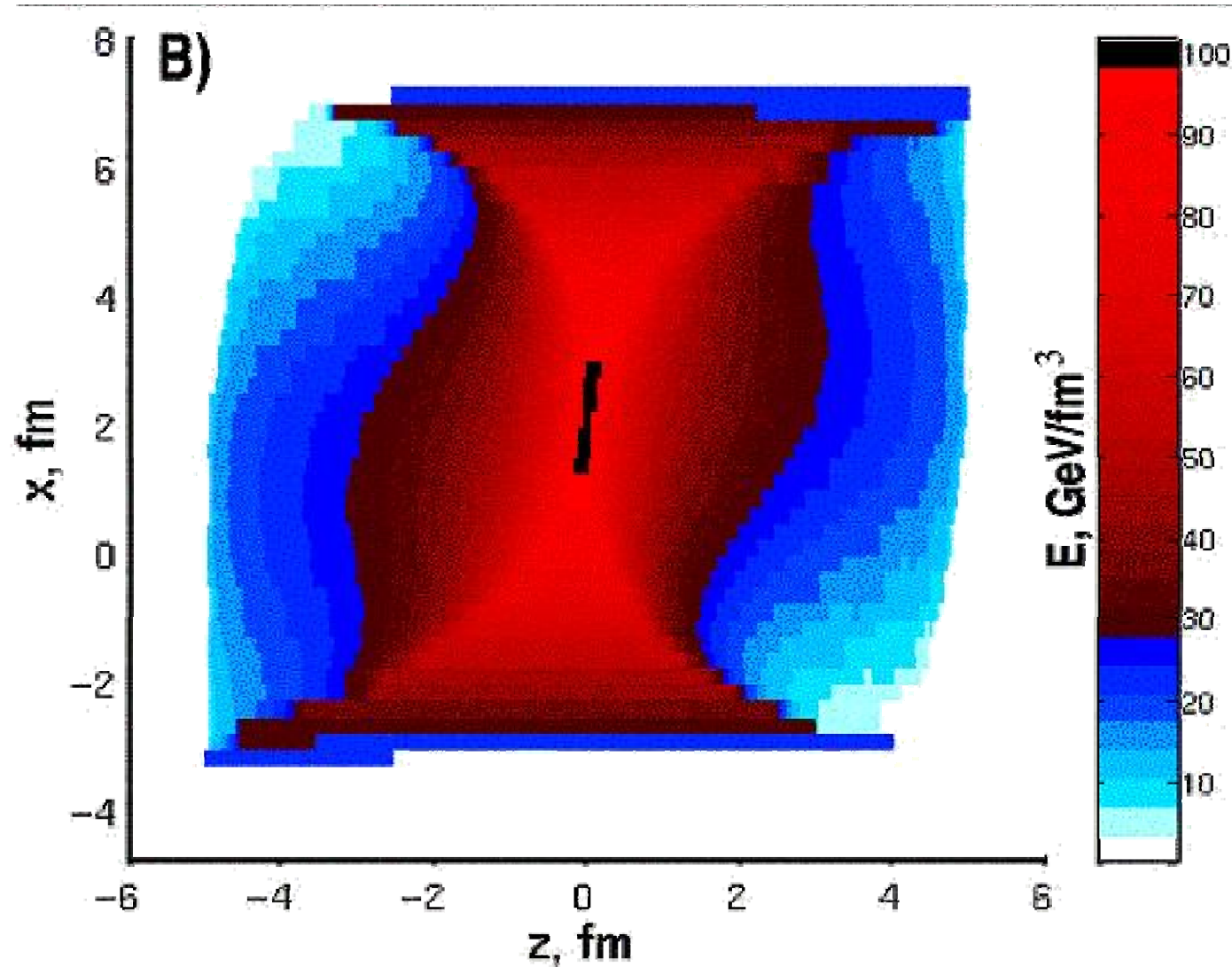
**Nuclei colliding at ultra-relativistic energies  
with nonzero impact parameter  
have a large initial angular momentum**



Symmetry axis = z-axis. Transverse plane divided into streaks

# Initial state from effective string rope model

Magas, Csernai, Strottman, PRC 64 (2001) 014901, NPA 712 (2002) 167

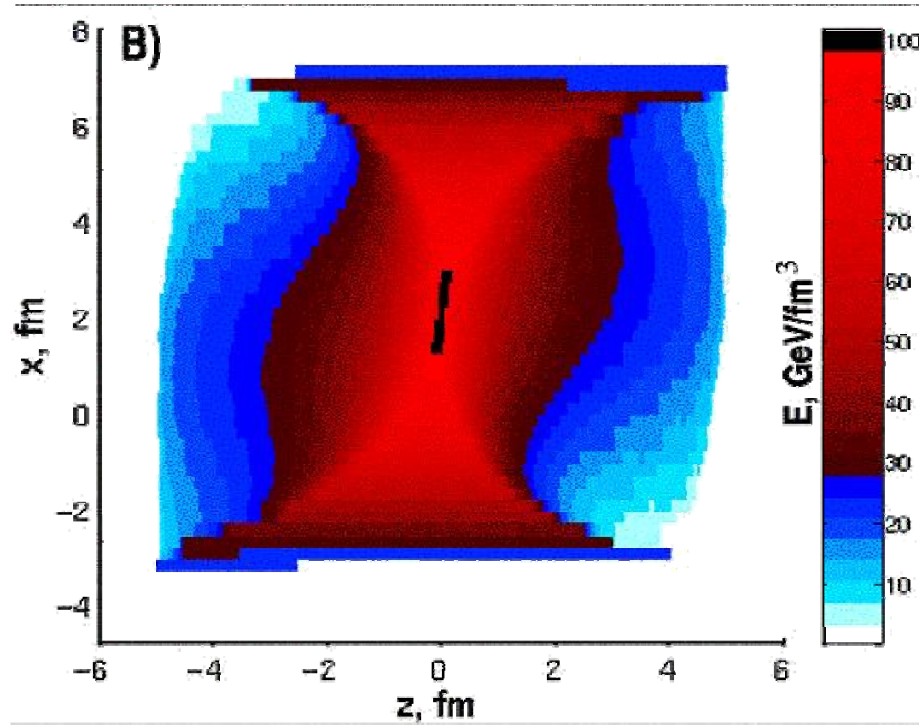


**Tilted!**

Au+Au at 100+100 GeV/nucl,  $b=0.25 \cdot 2R$

# Initial state from effective string rope model

Magas, Csernai, Strottman, PRC 64 (2001) 014901, NPA 712 (2002) 167



There are similar models,  
with different string decay mechanism,  
which produce  
initial state in  $(\tau, z)$  coordinates:

Mishustin, Kapusta,

**PRL 88 (2002) 112501;**

Mishustin, Lyakhov,

**Phys.Atom.Nucl. 75 (2012) 371**

Au+Au at 100+100 GeV/nucl,  $b=0.25*2R$

Initial State in  $(t, z)$  coordinate

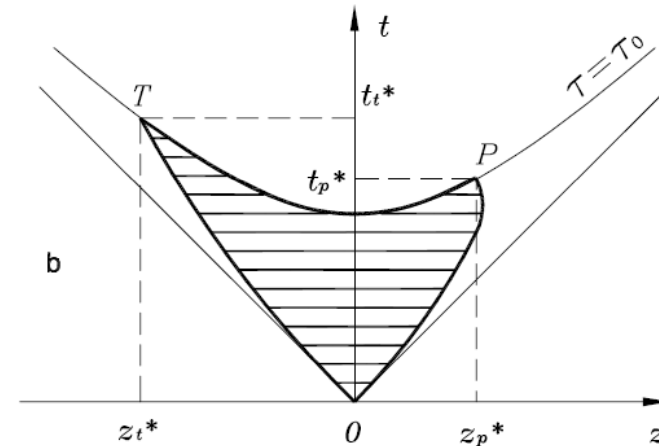


FIG. 2. Schematic space-time representation of a symmetric (a) and asymmetric (b) slab-slab collision in the  $t - z$  plane. The projectile and target slab trajectories are shown by thick solid lines which start at the origin and terminate at points P and T, respectively. The quark-gluon plasma is produced at the portion of the hyperbola  $\tau = \tau_0$  between these points (thick solid line). Horizontal solid lines represent strings. For symmetric collisions  $t_t^* = t_p^* = t^*$ ,  $z_t^* = -z_p^* = z^*$ .

3+1D hydro

Bjorken flow:  $u^\mu(\tau_0, x, y, \eta_{||}) = (\cosh \eta_{||}, 0, 0, \sinh \eta_{||})$ .

“Tilted” initial state:

$$\epsilon(\tau_0) = \epsilon_0 [2 (N_+(x, y) f_+(\eta_{||}) + N_-(x, y) f_-(\eta_{||})) (1 - \alpha) + 2\alpha N_{bin}(x, y) f(\eta_{||})] / N_0 . \quad (13)$$

where  $N_+$  and  $N_-$  are the densities of participants from the two colliding nuclei

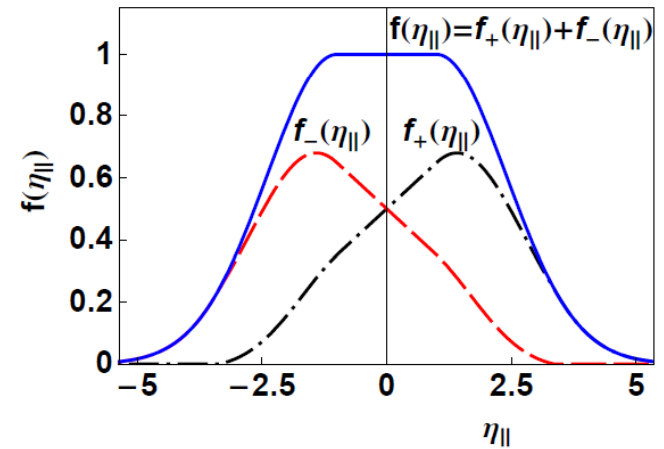


FIG. 2. (Color online) Initial profile in the longitudinal (space-time rapidity) direction. The symmetric function  $f(\eta_{||})$  is composed from two contributions  $f_+$  and  $f_-$  representing the emission from forward and backward going participant nucleons.

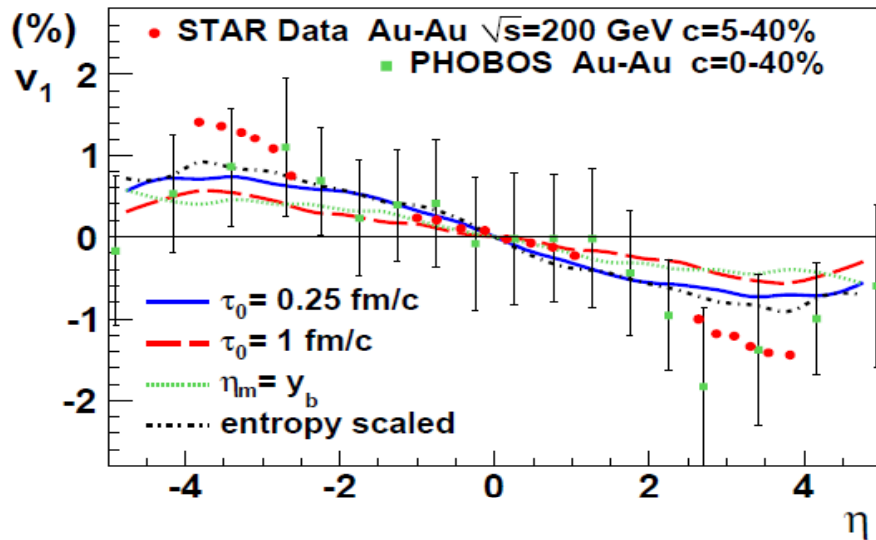
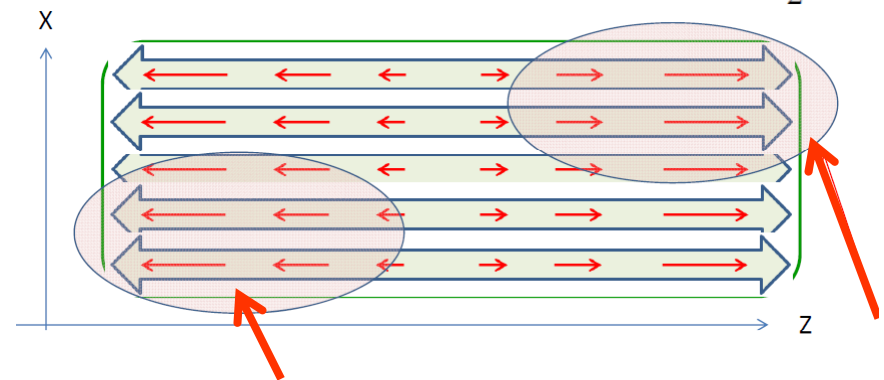


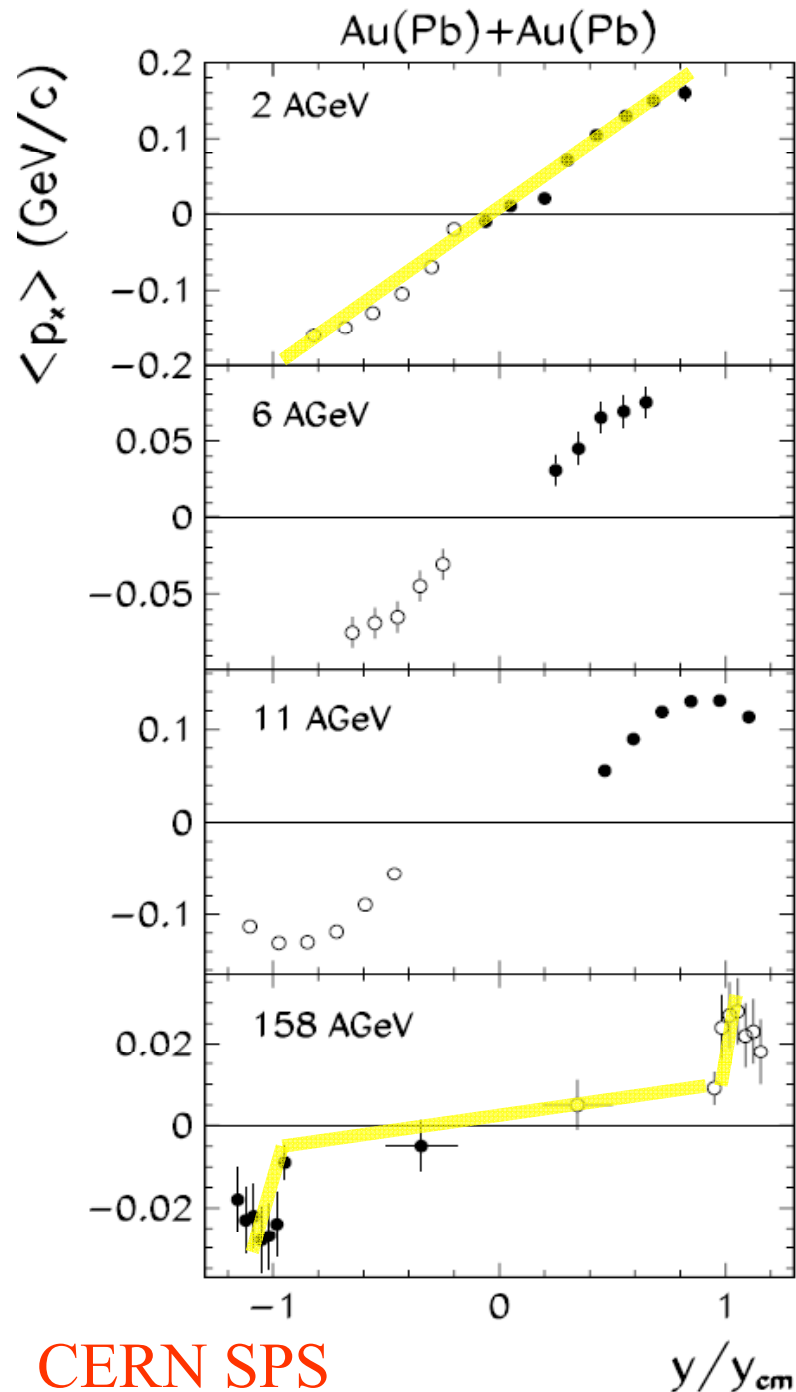
FIG. 9. (Color online) Directed flow coefficient as function of pseudorapidity for tilted initial conditions (Eq. 13) in Au-Au



*Matter is redistributed to the edges*

Which potential output such an initial state may have?

- Directed flow,  $v_1$
- Elliptic flow,  $v_2$
- Vorticity  $\Rightarrow$  particle polarization
- HBT



CERN SPS

Directed flow  
starts to deviate  
from straight line behavior:

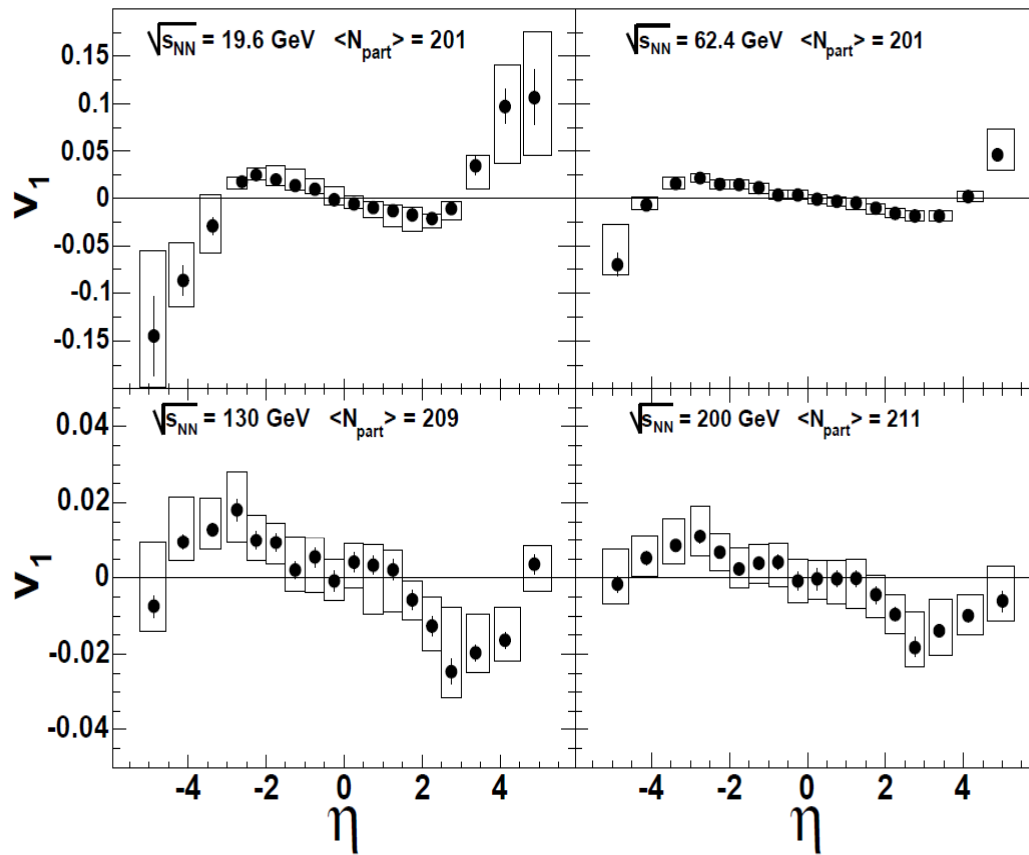
not just a simple **Bounce-off** -  
there is some matter  
accelerated by pressure

Antiflow or 3<sup>rd</sup> flow  
component

Was proposed as a possible  
QGP signal in

Csernai, Röhlich, PL B458 (1999) 454



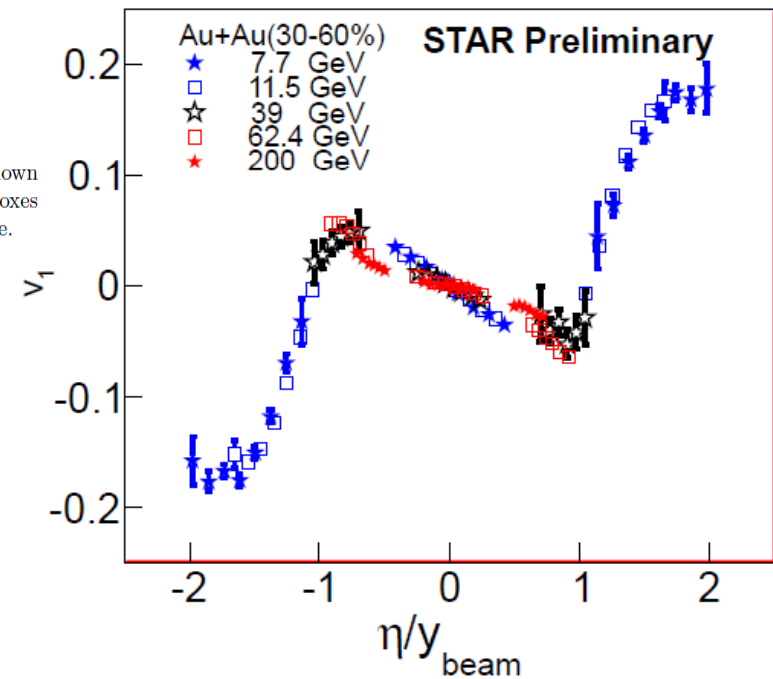


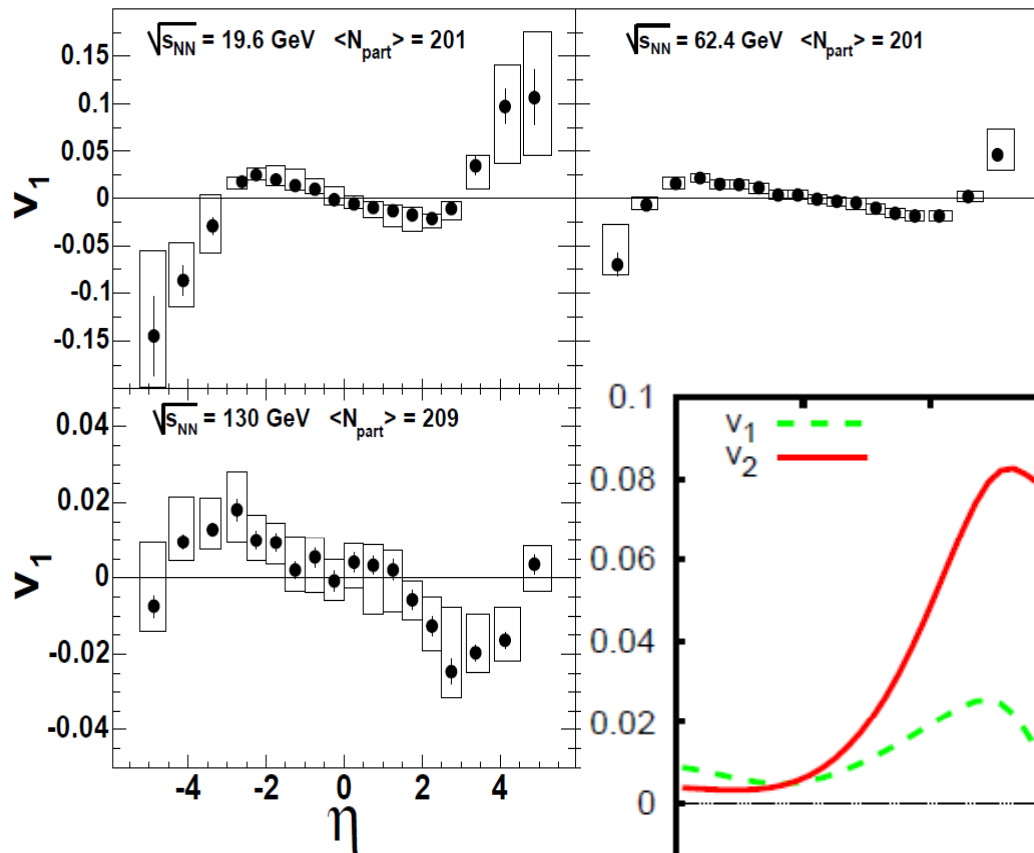
Strong antiflow in  $v_1$  is observed at RHIC

STAR Coll.  
Acta Phys.Polon.Supp. 5 (2012) 439

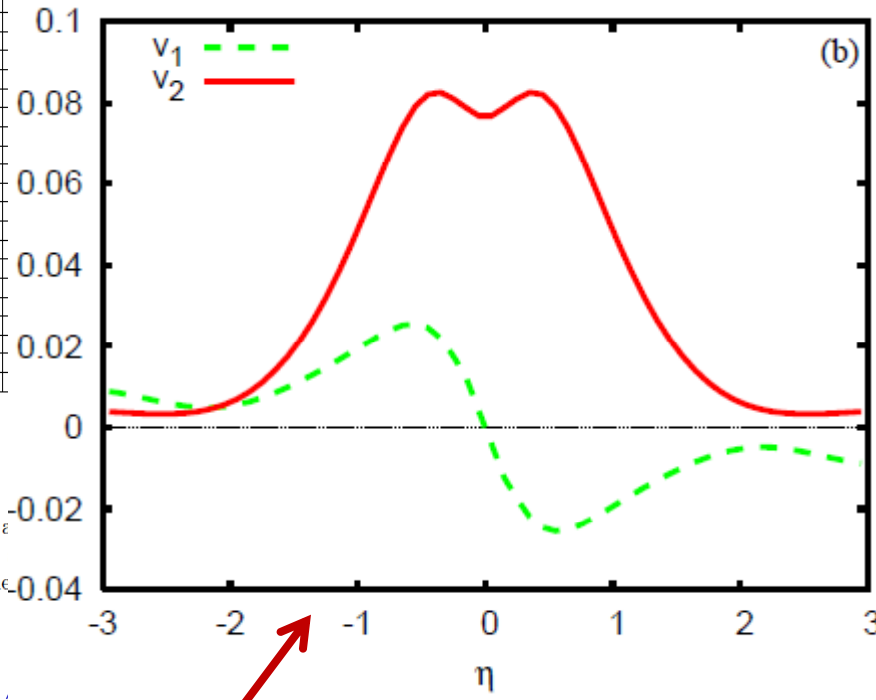
FIG. 2: Directed flow of charged particles in Au+Au collisions as a function of  $\eta$ , averaged over centrality (0-40%), shown separately for four beam energies. Note the different vertical axis scales between the upper and lower panels. The boxes represent systematic uncertainties at 90% C.L., and  $\langle N_{part} \rangle$  gives the average number of participants for each data sample.

PHOBOS Coll.  
Phys.Rev.Lett. 97 (2006) 012301





Strong antiflow in  $v_1$  is observed at RHIC



Phys. Rev. Lett. 103 (2012) 439

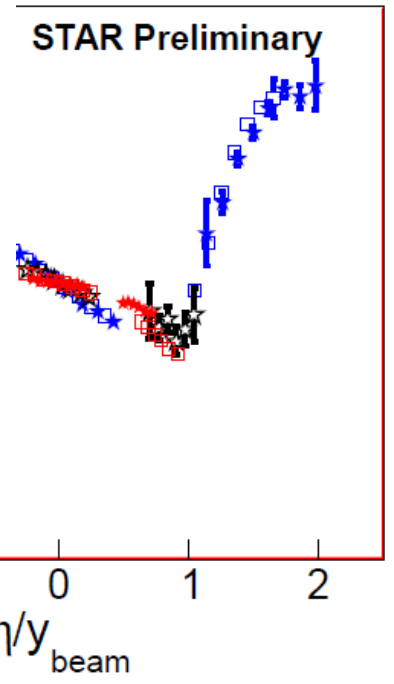
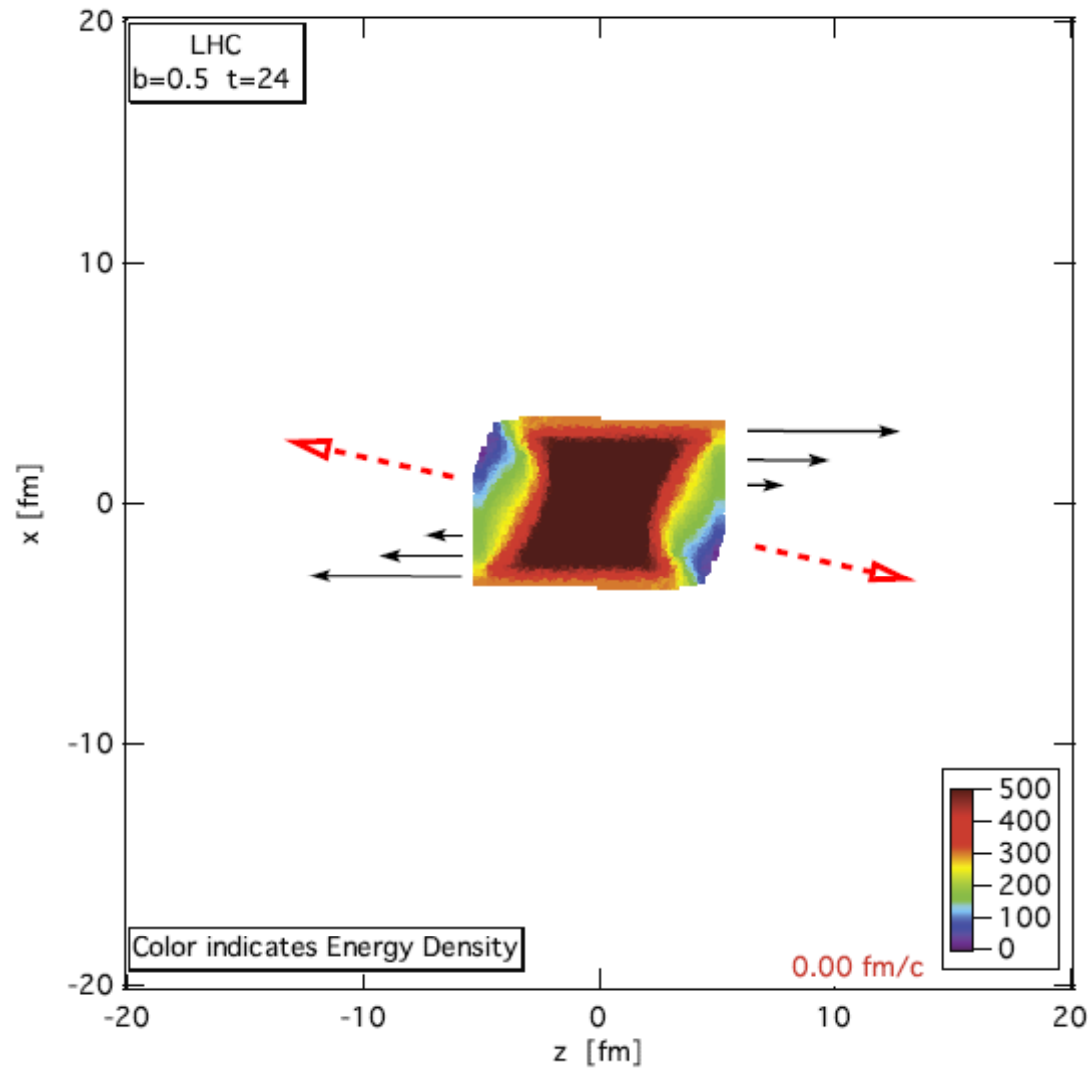


FIG. 2: Directed flow of charged particles in Au+Au collisions as a function of pseudorapidity  $\eta$  separately for four beam energies. Note the different vertical axis scales. The error bars represent systematic uncertainties at 90% C.L., and  $\langle N_{part} \rangle$  gives the average number of participants.

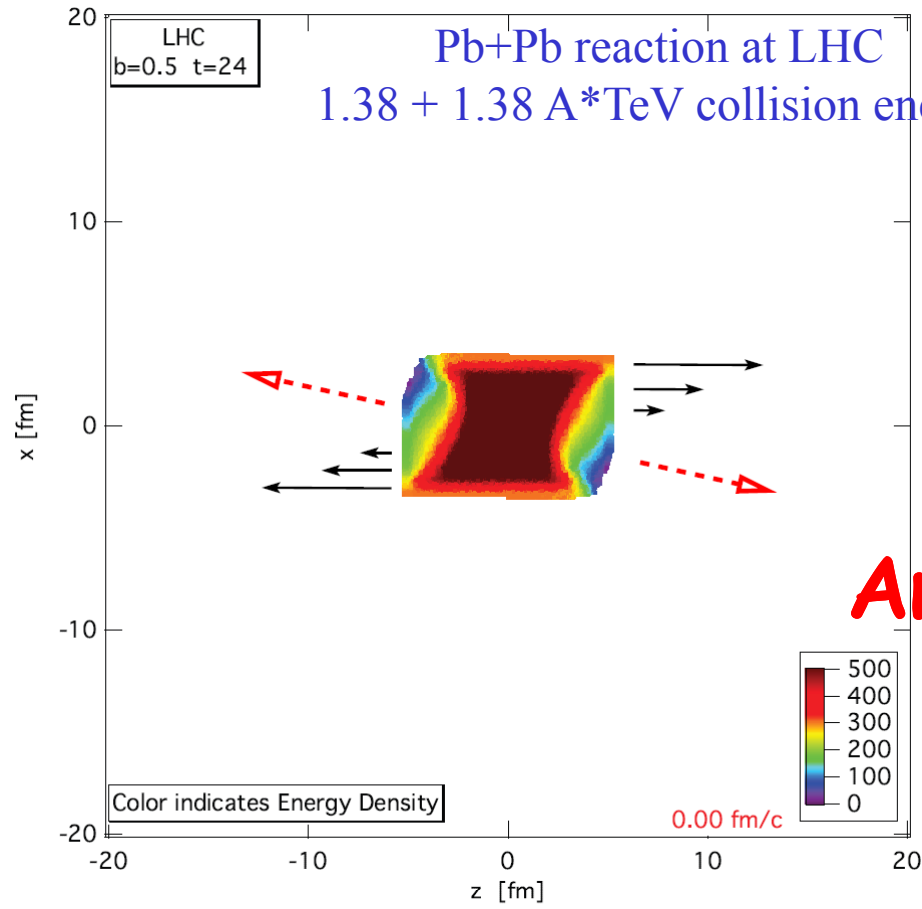
PHOBOS Coll.  
Phys.Rev.Lett. 97 (2006) 012301

Csernai et al, J. Phys. G34 (2007) S1077

Au+Au,  $\sqrt{s_{NN}} = 130$  GeV;  $b = 0.7 \cdot 2R_{Au}$

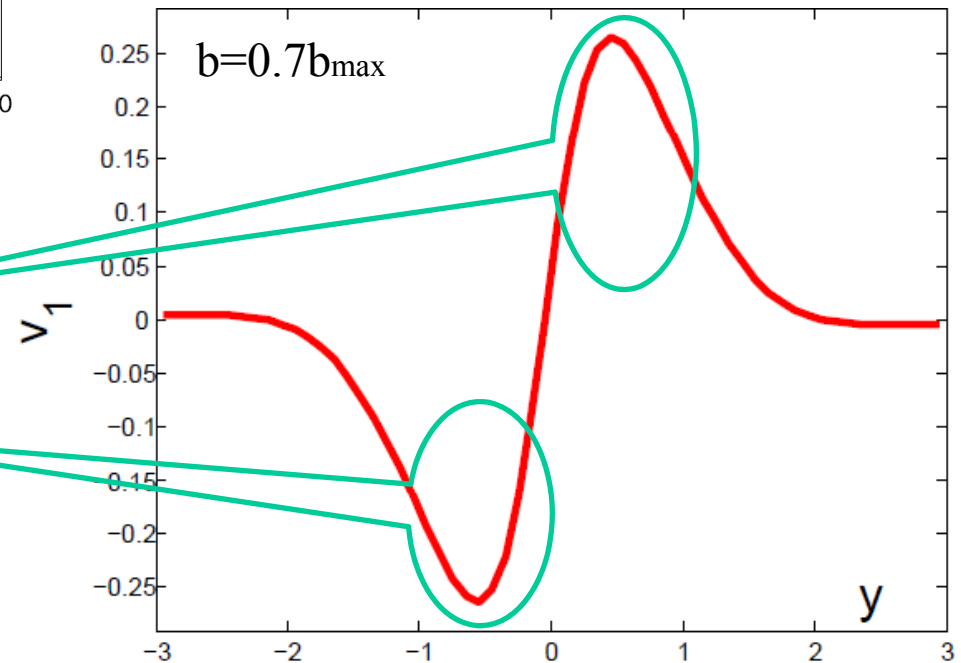


**Pb+Pb at 1.38 + 1.38 ATeV**  
Initial energy density [GeV/fm<sup>3</sup>]  
in the reaction plane  
 $b = 0.5_{bmax}$   
 $t=4$  fm/c after the first touch of  
the colliding nuclei



## Anti-flow ( $v_1$ ) at LHC

Peaks in opposite directions!!!  
What happened?

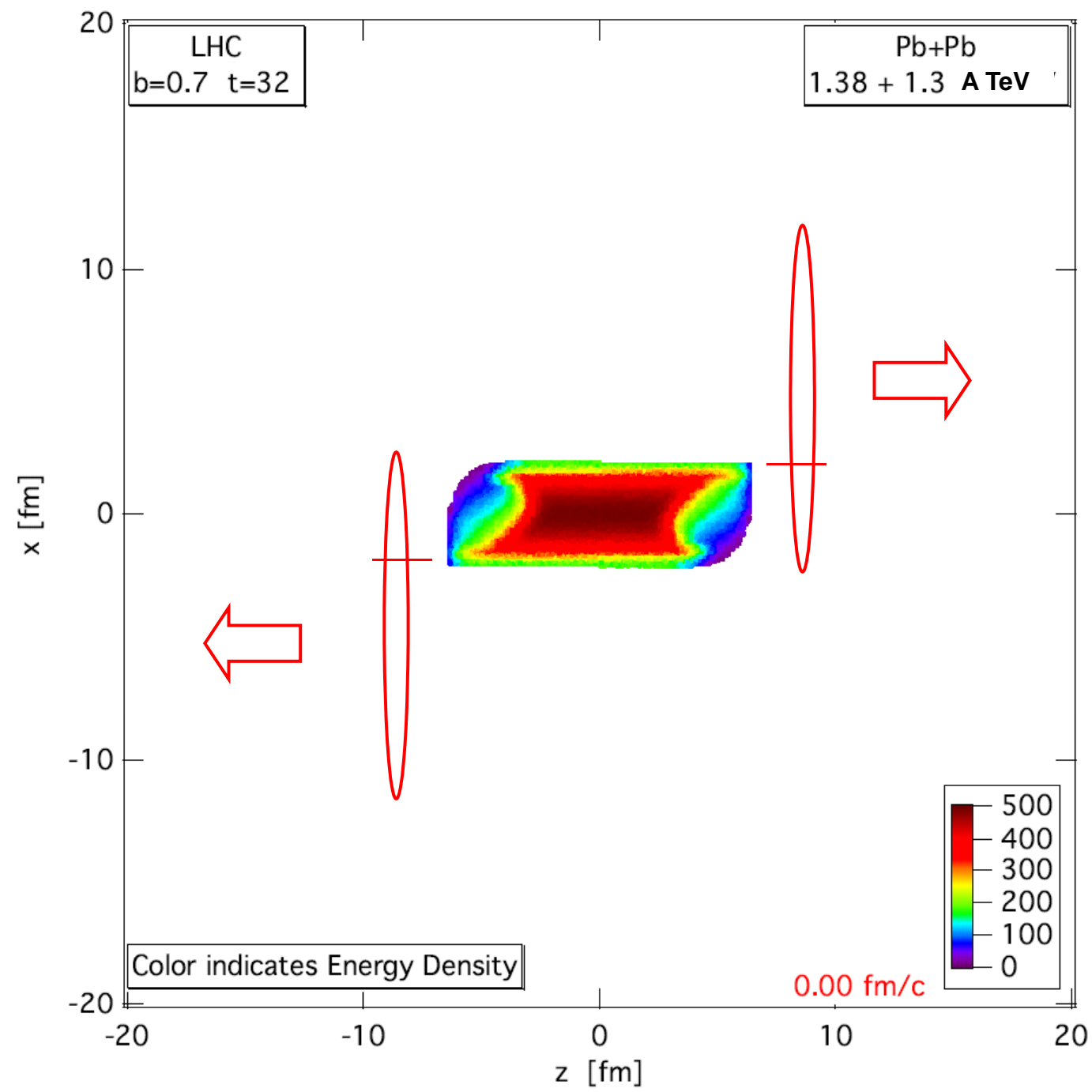


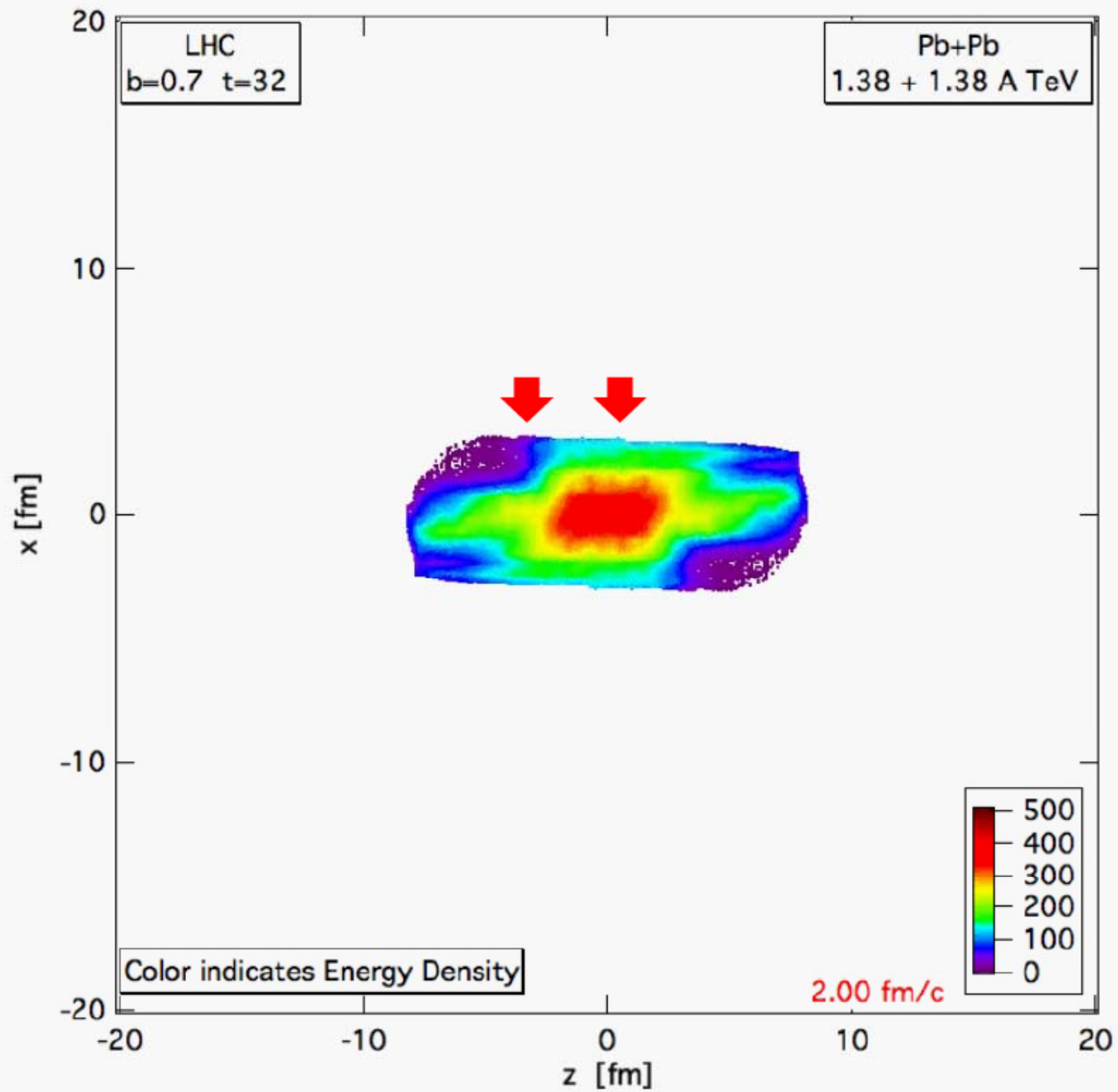
# PIC-hydro

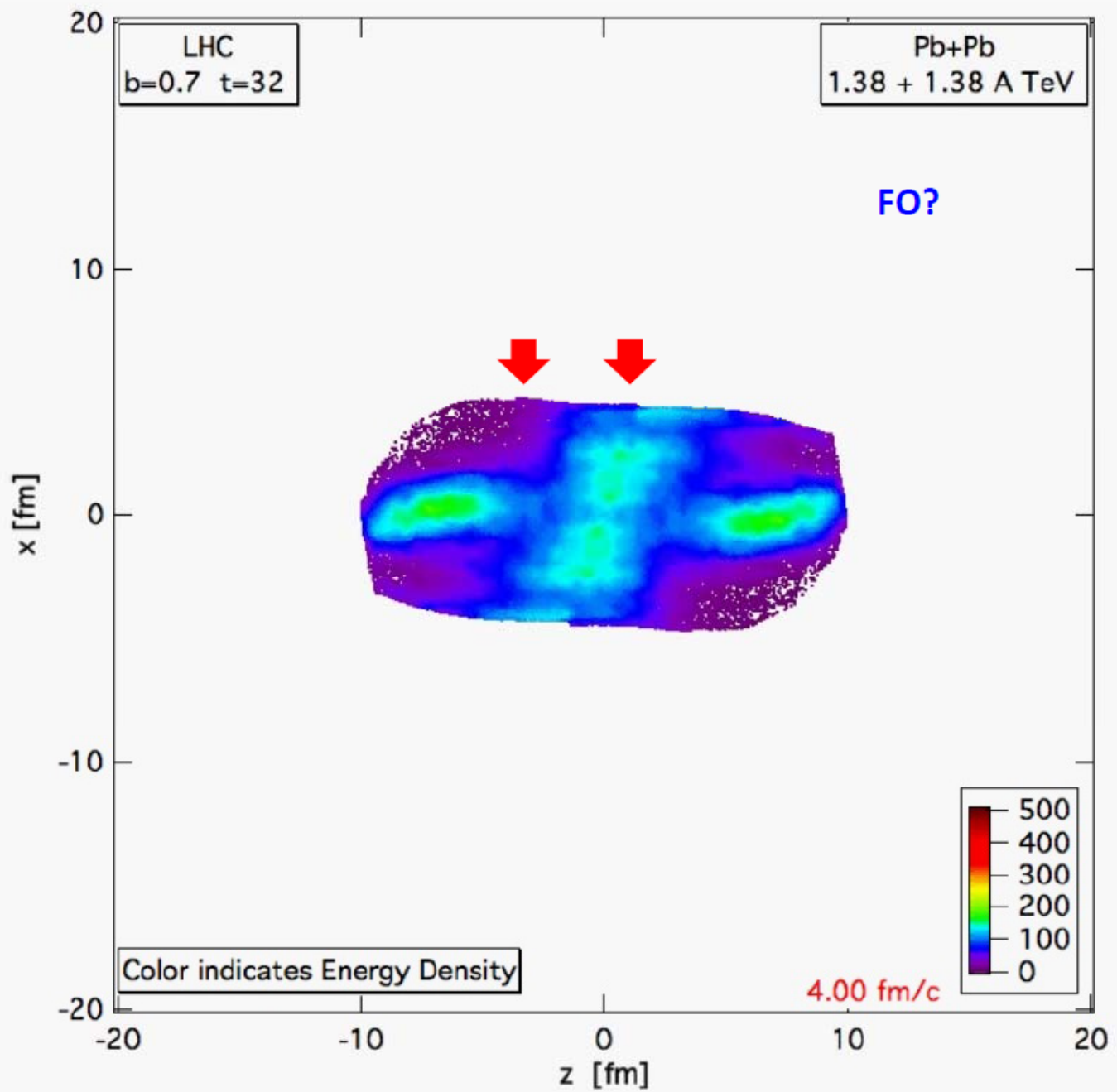
**Pb+Pb**  
**1.38+1.38 A TeV**  
 $b = 0.7b_{\text{max}}$

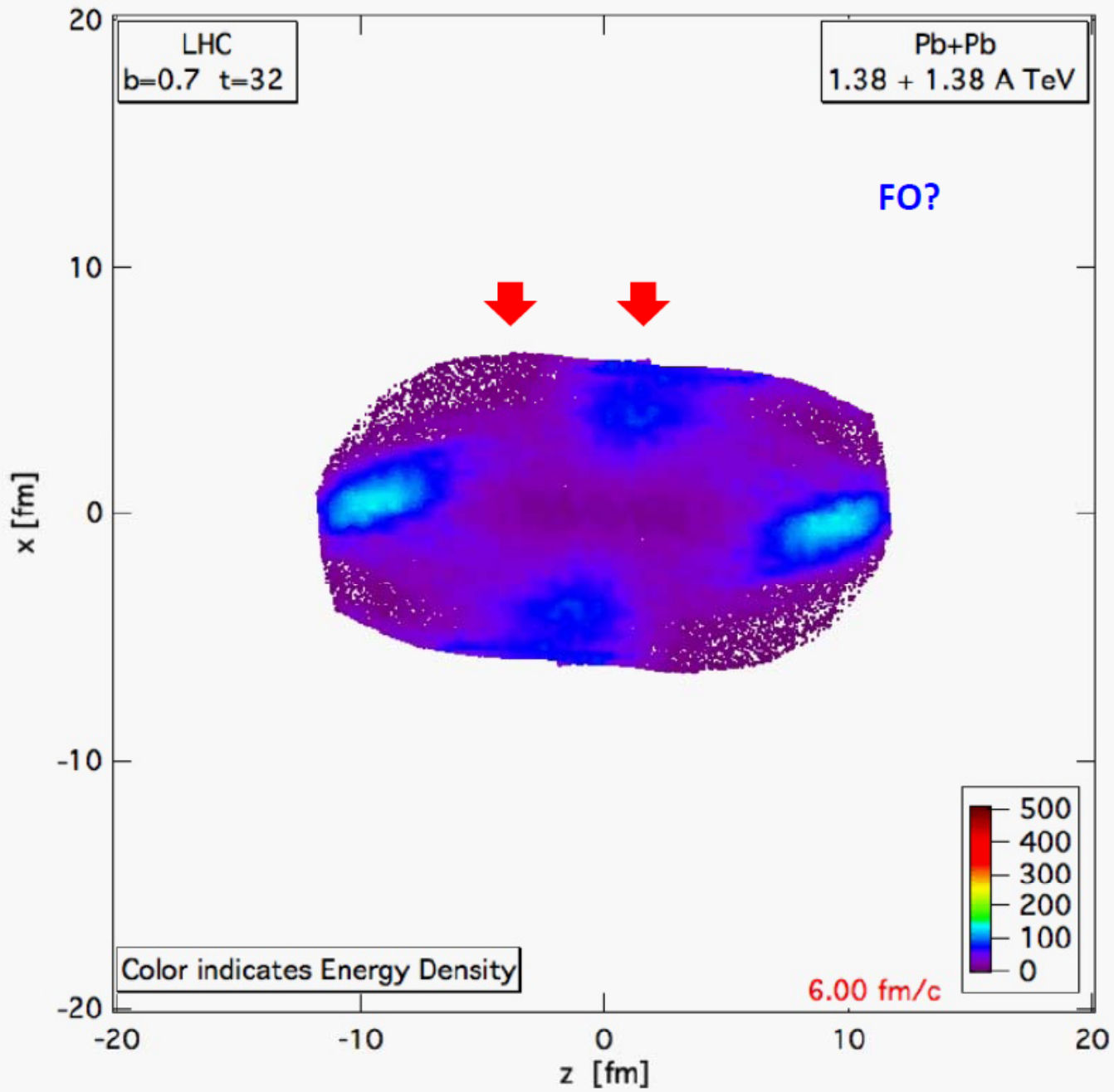
MIT Bag EoS  
FO:  $T \sim 200$  MeV  
but calculated much longer, until pressure is zero for 90% of the cells.

Structure and asymmetries of init. state are maintained in nearly perfect expansion.

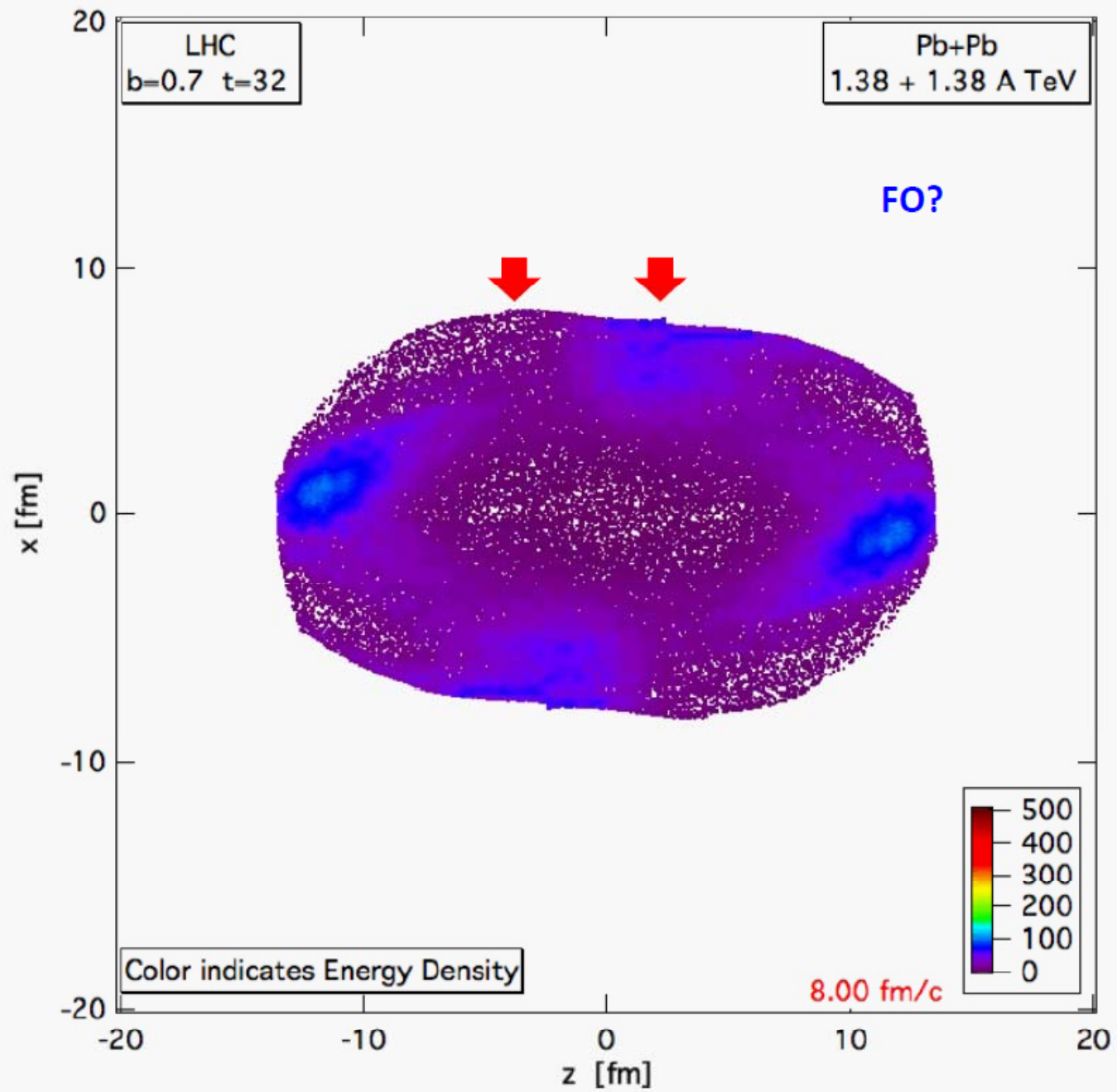


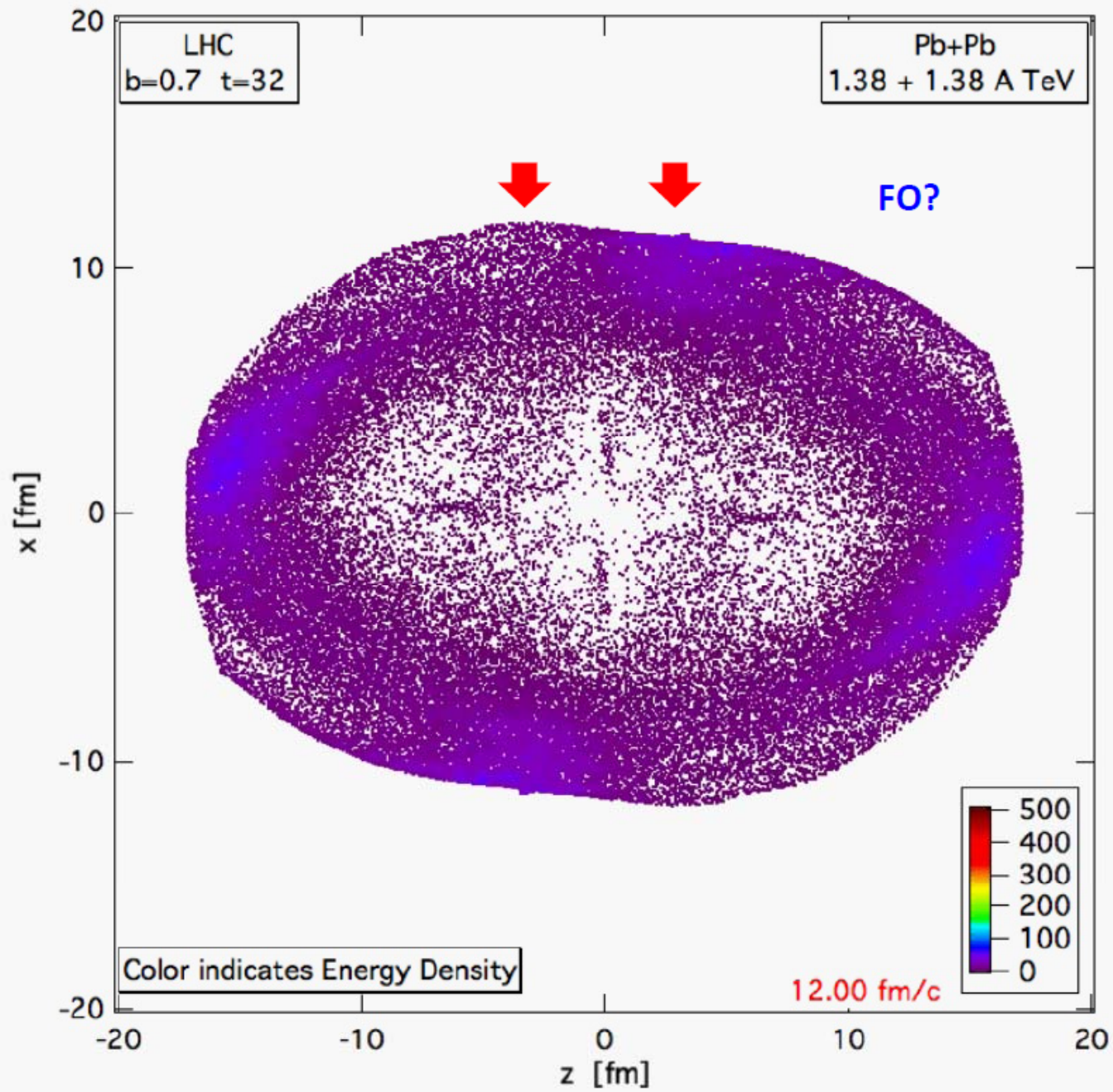


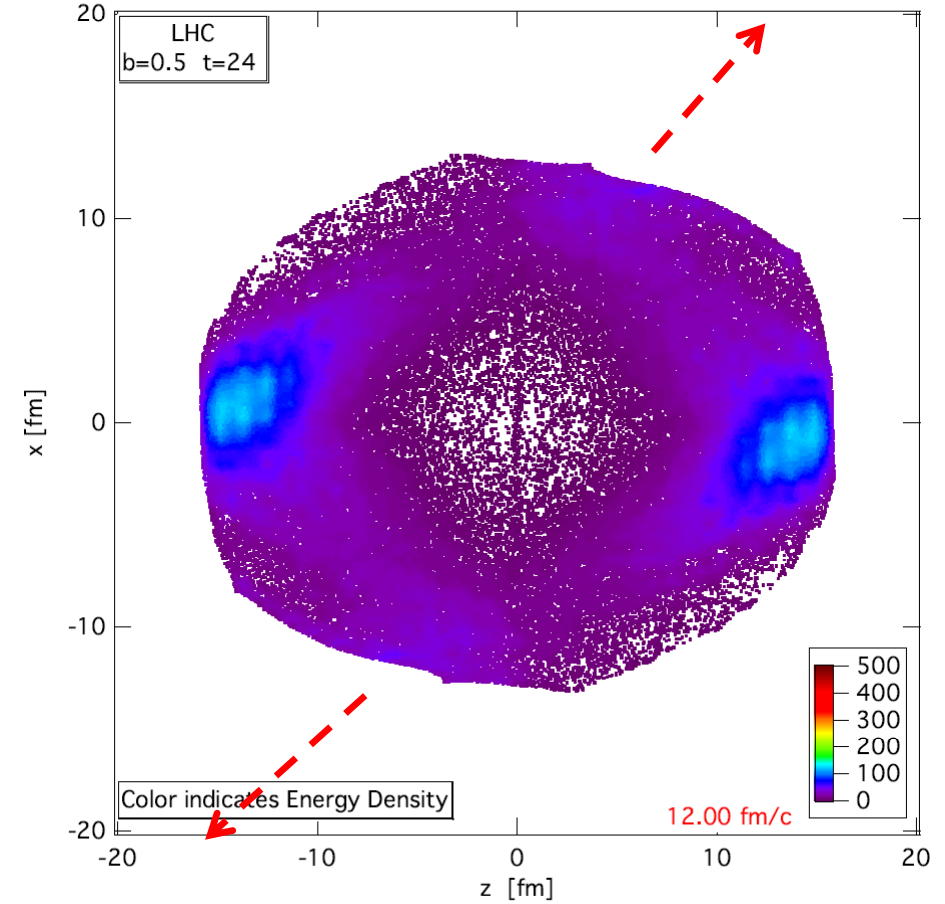
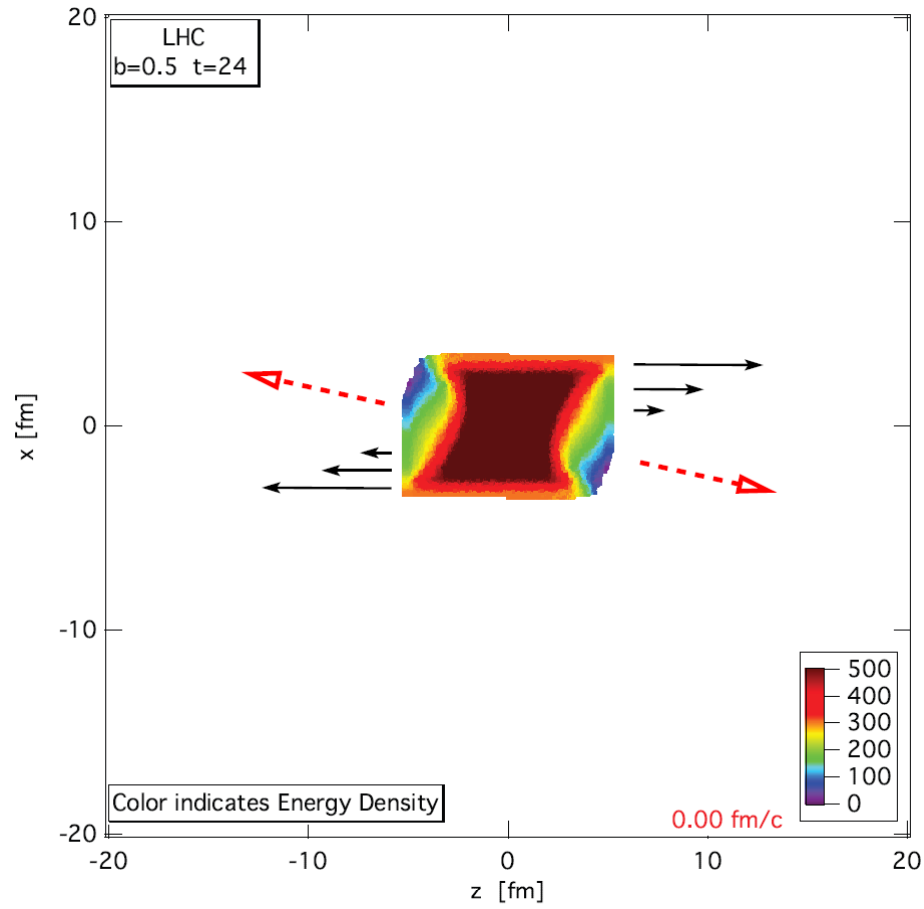






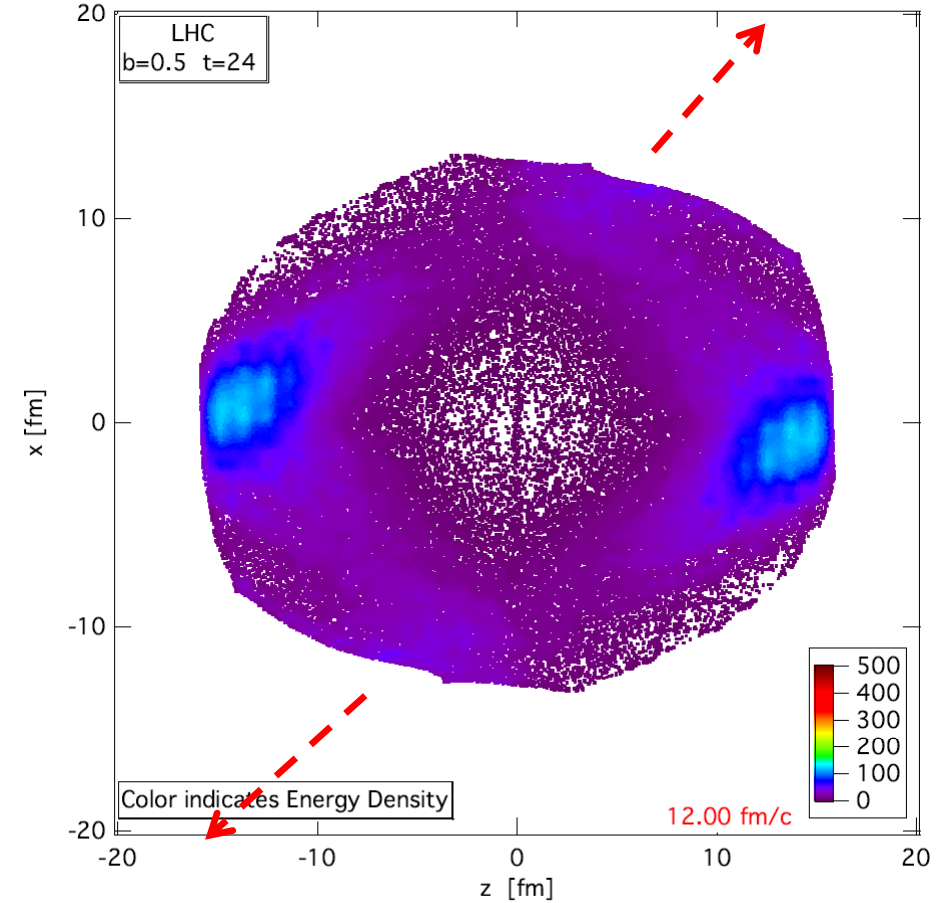
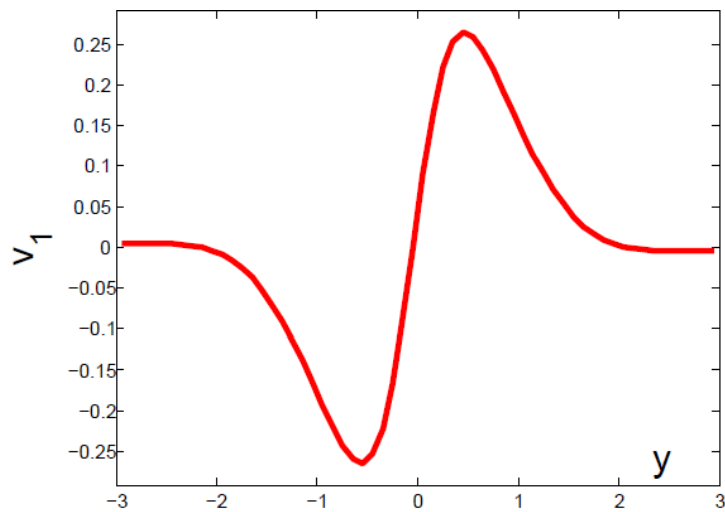
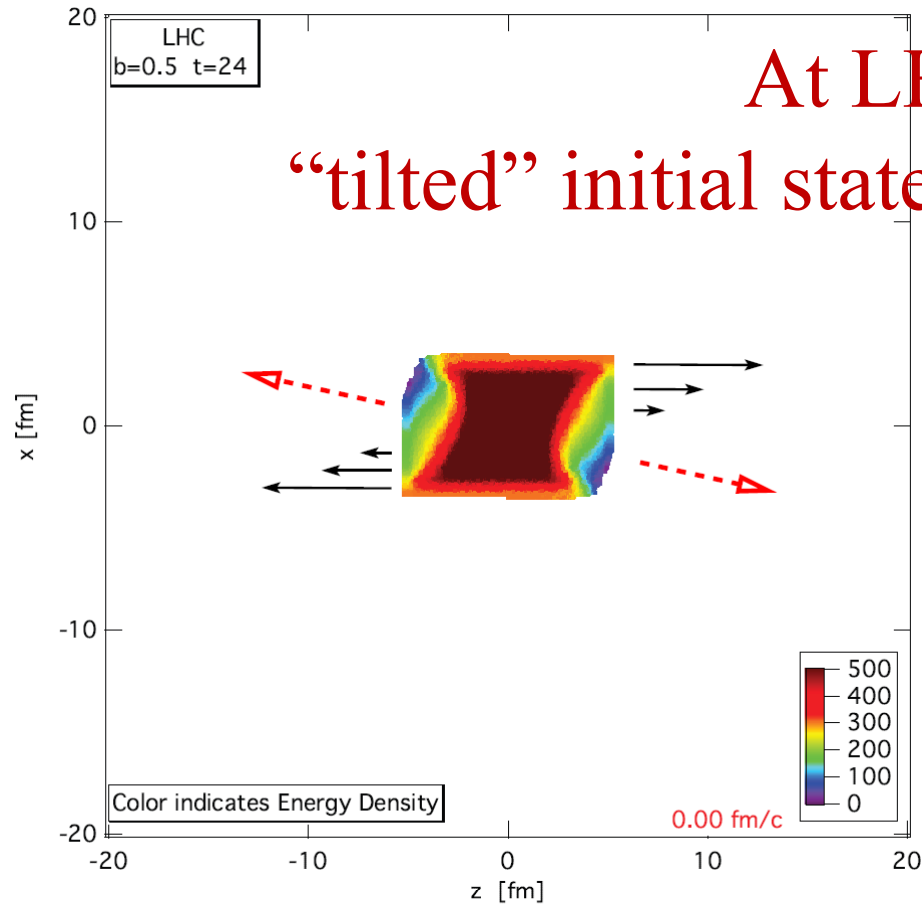




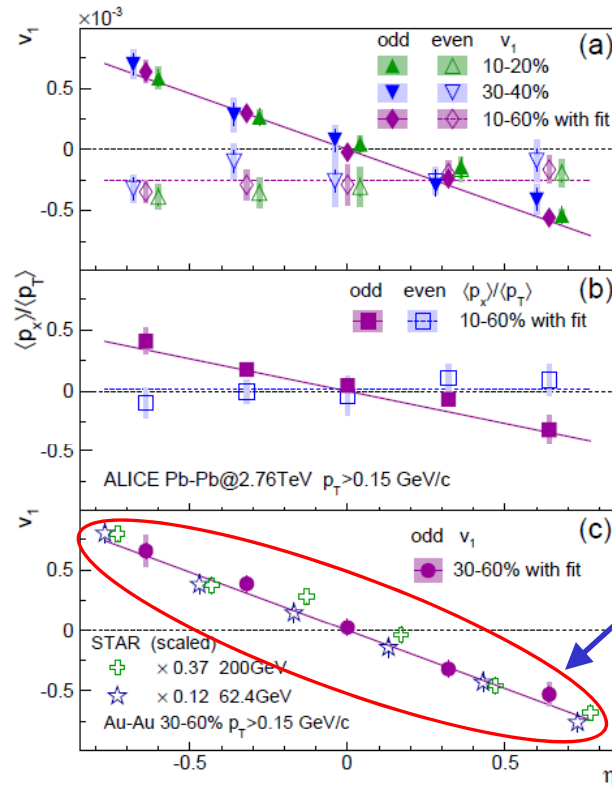


At LHC energies

“tilted” initial state  $\rightarrow$  “rotating” initial state



# ALICE Coll., arXiv: 1306.4145[nucl-ex]



$V_1$  at LHC  
has the same  
negative slope  
as at RHIC,  
but smaller  
magnitude

**Fig. 2:** (color online) (a)  $v_1$  and (b)  $\langle p_x \rangle / \langle p_T \rangle$  versus pseudorapidity in Pb-Pb collisions at  $\sqrt{s_{NN}} = 2.76$  TeV. The statistical (systematic) uncertainties are indicated by the error bars (shaded bands). Lines represent fits with linear (constant) function for  $v_1^{\text{odd}}$  ( $v_1^{\text{even}}$ ). (c)  $v_1^{\text{odd}}$  in Pb-Pb collisions compared to the STAR data [32] for Au-Au collisions at  $\sqrt{s_{NN}} = 200$  (62.4) GeV downscaled with a factor 0.37 (0.12).

$V_1$  consistent with ideal hydrodynamic model calculations for **dipole-like energy fluctuations** in the overlap zone:

Gardim et al., PRC83, 064901 (2011);

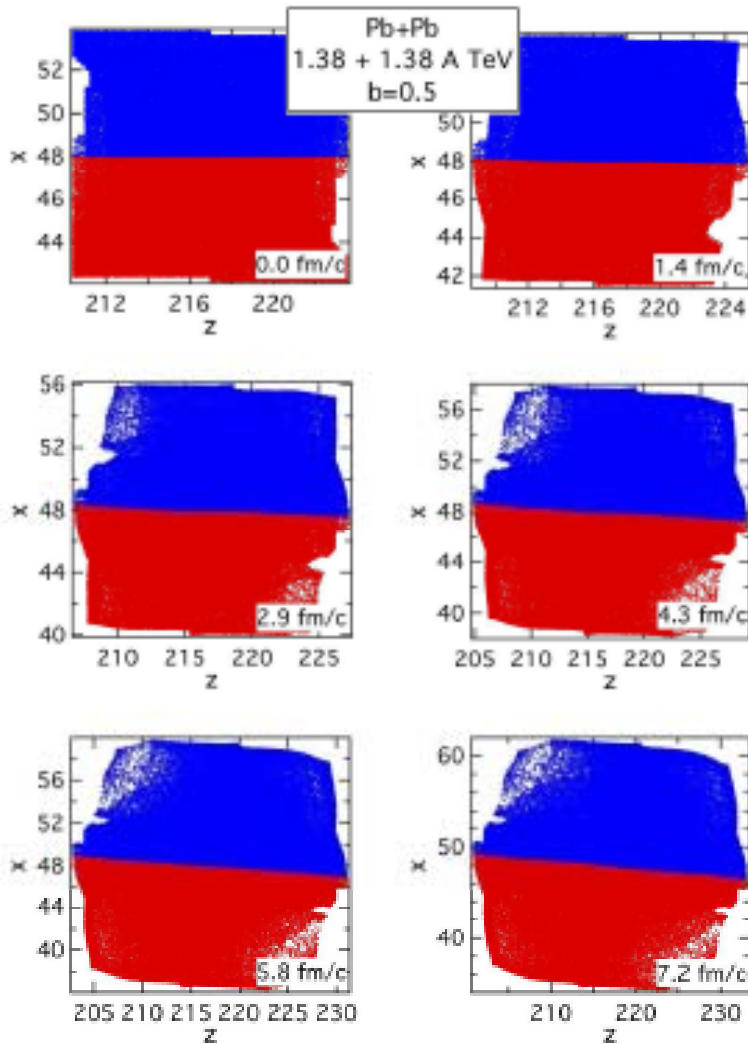
Retinskaya, Luzum, Ollitrault, PRL108, 252302 (2012)

Kelvin-Helmholtz instability in high-energy heavy-ion collisions

L.P. Csernai<sup>1,2,3</sup>, D.D. Strottman<sup>2,3</sup>, and Cs. Anderlik<sup>4</sup>

PHYSICAL REVIEW C **85**, 054901 (2012)

## ROTATION



KHI →

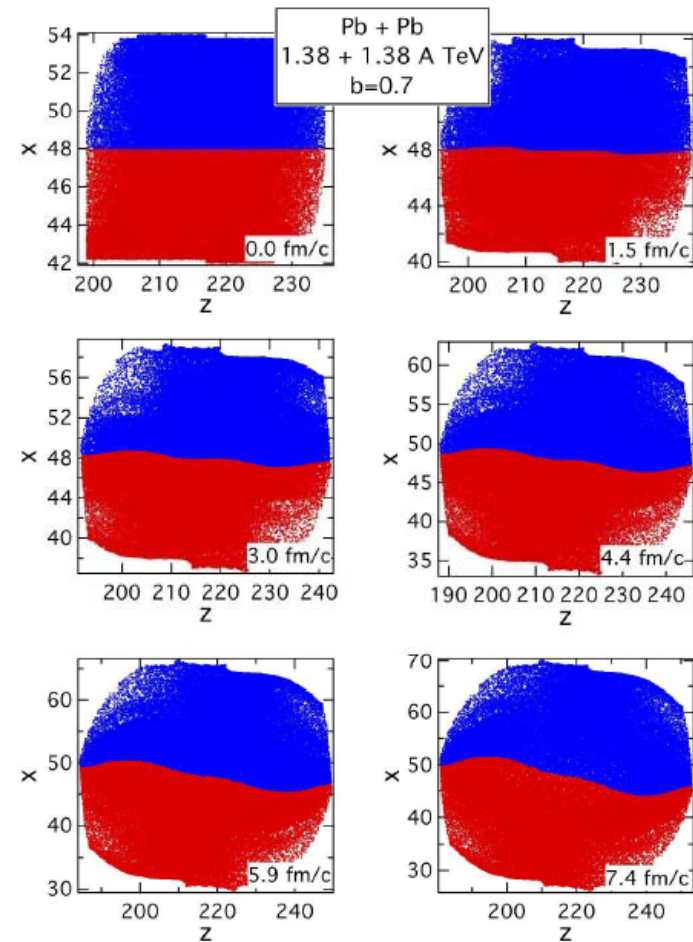


FIG. 1: (color online) Growth of the initial stage of Kelvin-Helmholtz instability in a  $1.38A + 1.38A$  TeV peripheral,  $b = 0.7b_{\text{max}}$ , Pb+Pb collision in a relativistic CFD simulation using the PIC-method. We see the positions of the marker particles (Lagrangian markers with fixed baryon number content) in the reaction plane. The calculation cells are  $dx = dy = dz = 0.4375\text{fm}$  and the time-step is  $0.04233 \text{ fm}/c$ . The number of randomly placed marker particles in each fluid cell is  $8^3$ . The axis-labels indicate the cell numbers in the  $x$  and  $z$  (beam) direction. The initial development of a KH type instability is visible from  $t = 1.5$  up to  $t = 7.41 \text{ fm}/c$  corresponding from 35 to 175 calculation time steps).

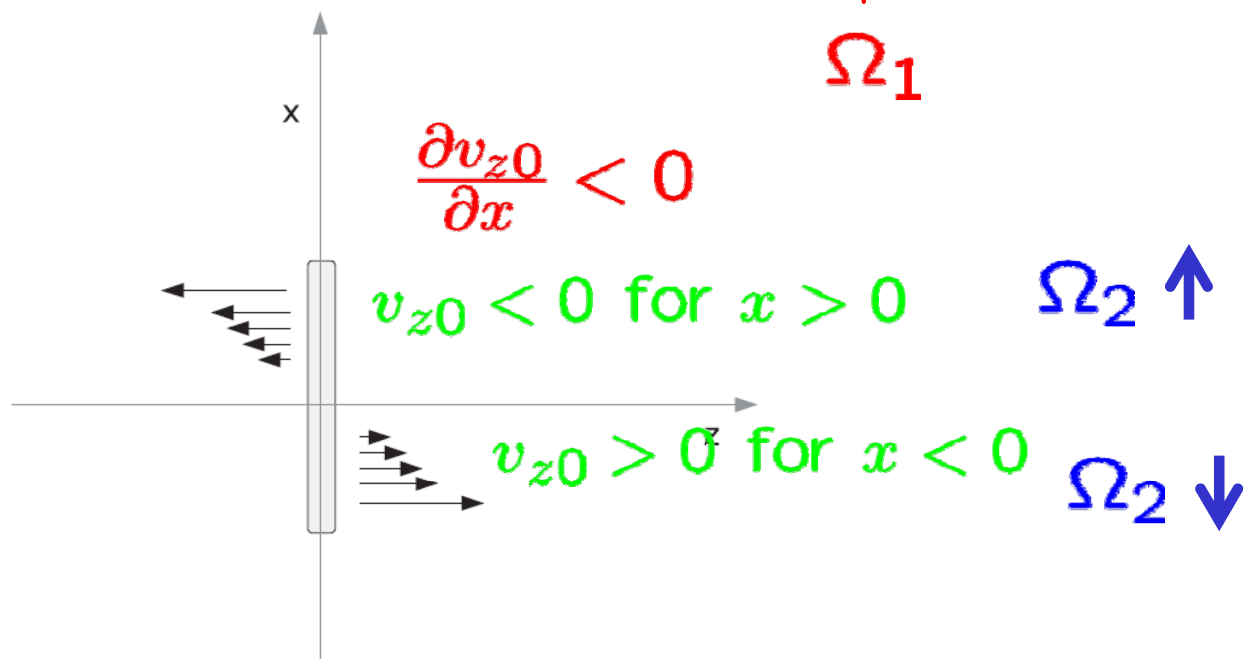
# Elliptic flow from rotating initial state

## Euler equation

$$(e + P)(\mathbf{u} \cdot \partial)\mathbf{u}^\mu = g^{\mu\nu} \partial_\nu P - (\mathbf{u} \cdot \partial P)\mathbf{u}^\mu$$

$$t = 0 : v_x = v_y = 0, \gamma_0^2 = 1/(1 - v_{z0}^2); P = e/3$$

$$e_0 \gamma_0^3 \frac{\partial u_i}{\partial t} \Big|_{t=0} = \underbrace{-\frac{1}{4} \frac{\partial e \gamma^2}{\partial x_i} \Big|_{t=0}}_{\Omega_1} + \underbrace{\frac{1}{4} 2e_0 \gamma_0^4 v_{z0} \frac{\partial v_{z0}}{\partial x_i} \Big|_{t=0}}_{\Omega_2}$$

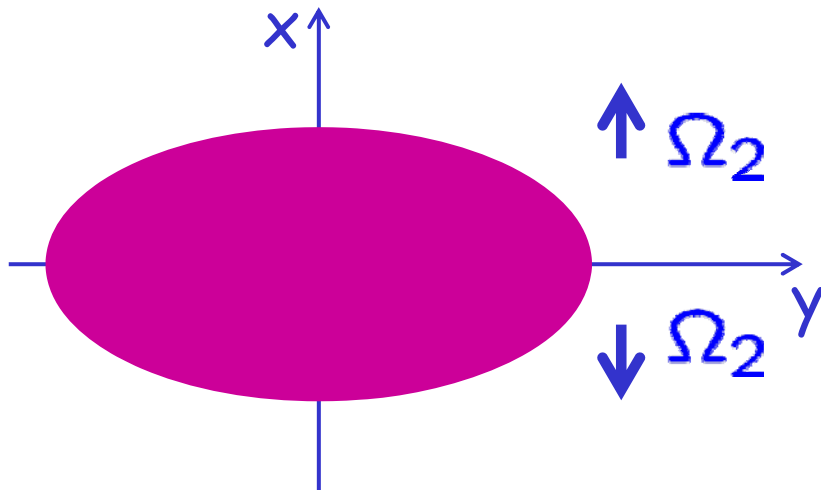


# Elliptic flow from rotating initial state

## Euler equation

$$e_0 \gamma_0^3 \frac{\partial u_i}{\partial t} \Big|_{t=0} = \underbrace{-\frac{1}{4} \frac{\partial e \gamma^2}{\partial x_i} \Big|_{t=0}}_{\Omega_1} + \underbrace{\frac{1}{4} 2 e_0 \gamma_0^4 v_{z0} \frac{\partial v_{z0}}{\partial x_i} \Big|_{t=0}}_{\Omega_2}$$

$$\left| \frac{\partial v_{z0}}{\partial x} \right| > \left| \frac{\partial v_{z0}}{\partial y} \right|$$



$\Omega_2$  helps  
to produce  
elliptic flow!



# Simple toy model initial state

Becattini, Piccinini, Rizzo, **PRC 77, 024906 (2008)**

## Landau disc

but with initial flow velocity  $\mathbf{v}_z$

$$J = - \int d^3\vec{r} x T^{0z} = - \int d^3\vec{r} x (e + P) \gamma^2 v_z(x)$$

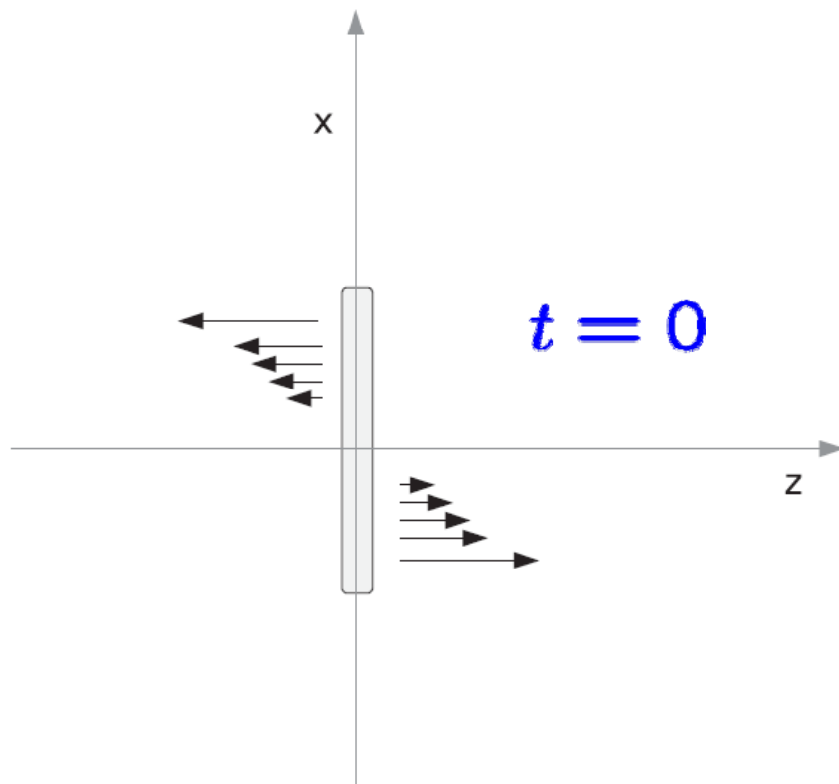


FIG. 4. Initial longitudinal velocity profile for the limiting case of sudden thermalization in the very thin overlap region of the colliding ultrarelativistic nuclei.

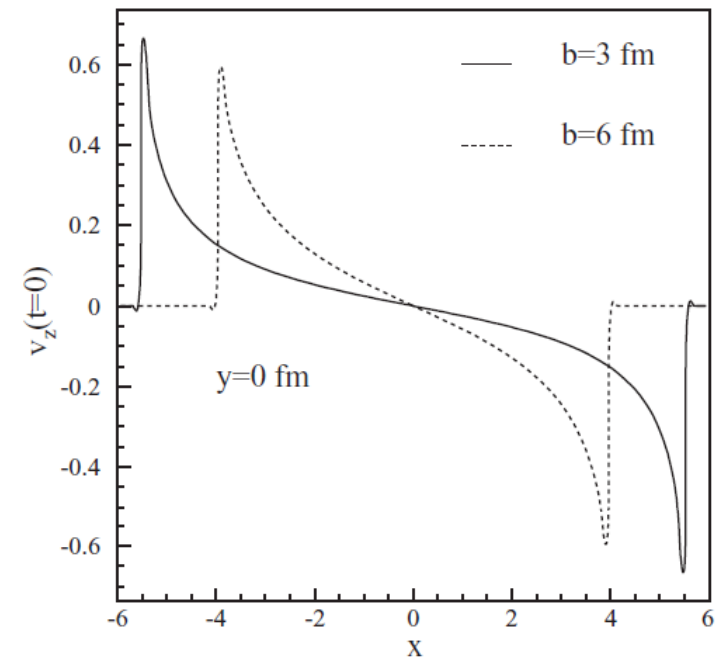


FIG. 5. Initial longitudinal velocity profile along the reaction plane  $y = 0$  for two different impact parameters for the collision of two hard-sphere nuclei with 7-fm radius.

# Simple toy model initial state

Becattini, Piccinini, Rizzo, **PRC 77, 024906 (2008)**

**Landau disc**  
but with initial flow velocity  $\mathbf{v}_z$

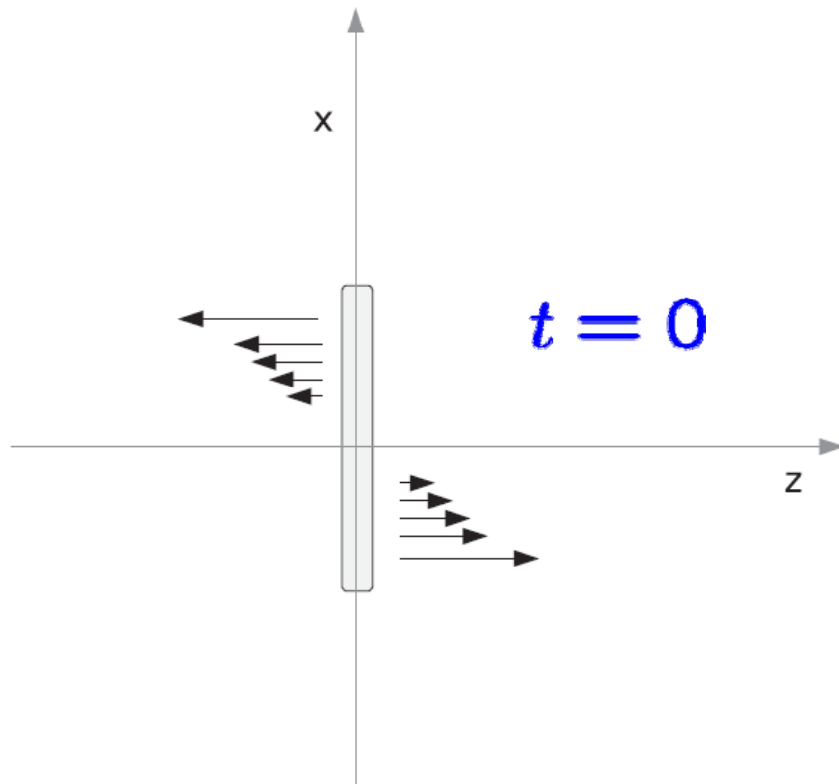


FIG. 4. Initial longitudinal velocity profile for the limiting case of sudden thermalization in the very thin overlap region of the colliding ultrarelativistic nuclei.

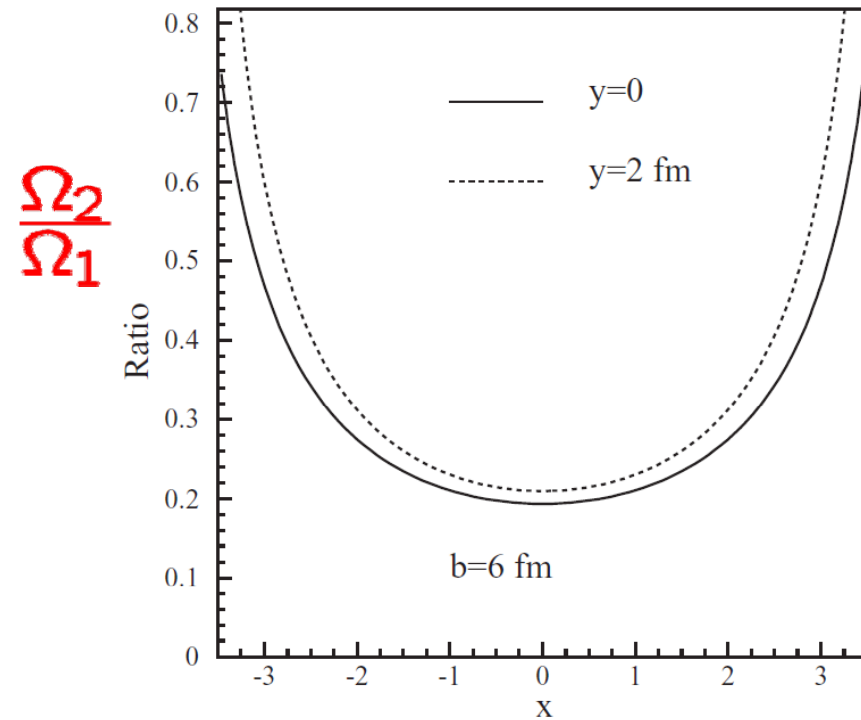


FIG. 6. Ratio of the term proportional to the vorticity and the term proportional to energy density gradient along  $x$  in Eq. (16) as a function of  $x$  for  $y = 0$  and  $y = 2$  fm for the collision of two hard-sphere nuclei with 7-fm radius at an impact parameter  $b = 6$  fm.

## Elliptic flow from spinning system

$$v_2^{(J)} = \frac{\int d^3x \frac{K_1\left(m_T \sqrt{1-|\boldsymbol{\omega} \times \mathbf{x}|_{\parallel}^2}/T\right)}{\sqrt{1-|\boldsymbol{\omega} \times \mathbf{x}|_{\parallel}^2}} I_2\left(\frac{p_T z \omega}{T}\right)}{\int d^3x \frac{K_1\left(m_T \sqrt{1-|\boldsymbol{\omega} \times \mathbf{x}|_{\parallel}^2}/T\right)}{\sqrt{1-|\boldsymbol{\omega} \times \mathbf{x}|_{\parallel}^2}} I_0\left(\frac{p_T z \omega}{T}\right)}$$

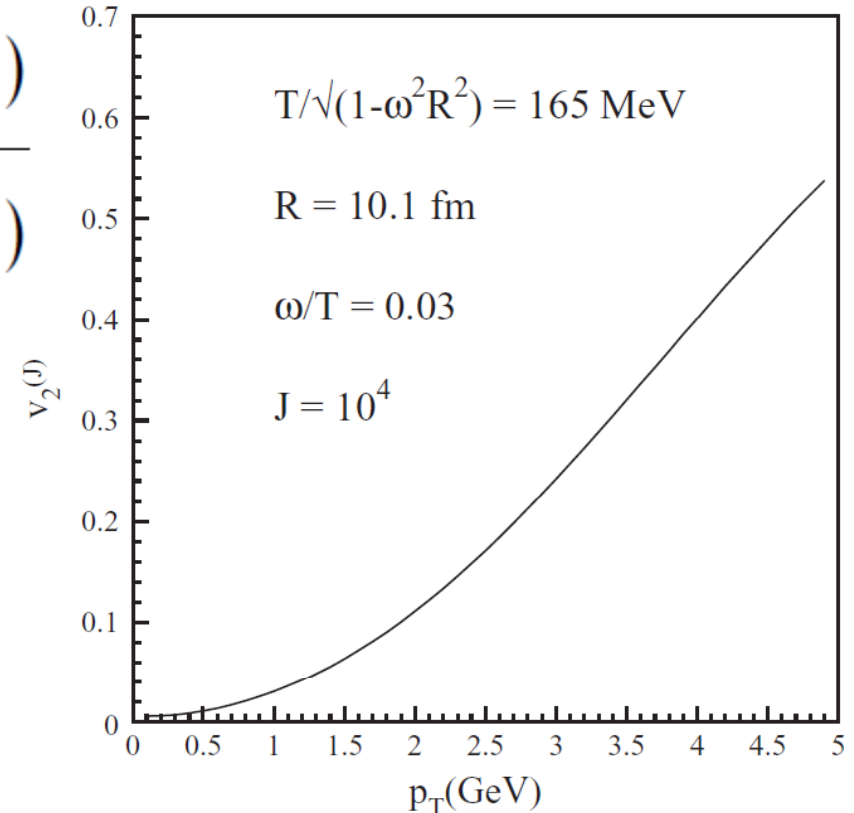


FIG. 7. Elliptic flow coefficient  $v_2^{(J)}$  as a function of  $p_T$  for hadrons originated from a spherical spinning plasma at a chemical freeze-out  $T = 165 \text{ MeV}$  and a radius of  $10.1 \text{ fm}$  for  $\omega/T = 0.03$ . The elliptic flow would simply vanish if  $J = 0$ .

# Flow Vorticity

Classical

$$\boldsymbol{\omega} \equiv \frac{1}{2} \text{rot } \boldsymbol{v} = \frac{1}{2} \nabla \times \boldsymbol{v}$$

$$\Omega_{zx} \equiv w(z, x) \quad \omega_{zx}$$

energy density weighted  
vorticity

Relativistic

$$\omega_{\mu\nu} = \frac{1}{2} (\partial_\nu u_\mu - \partial_\mu u_\nu)$$

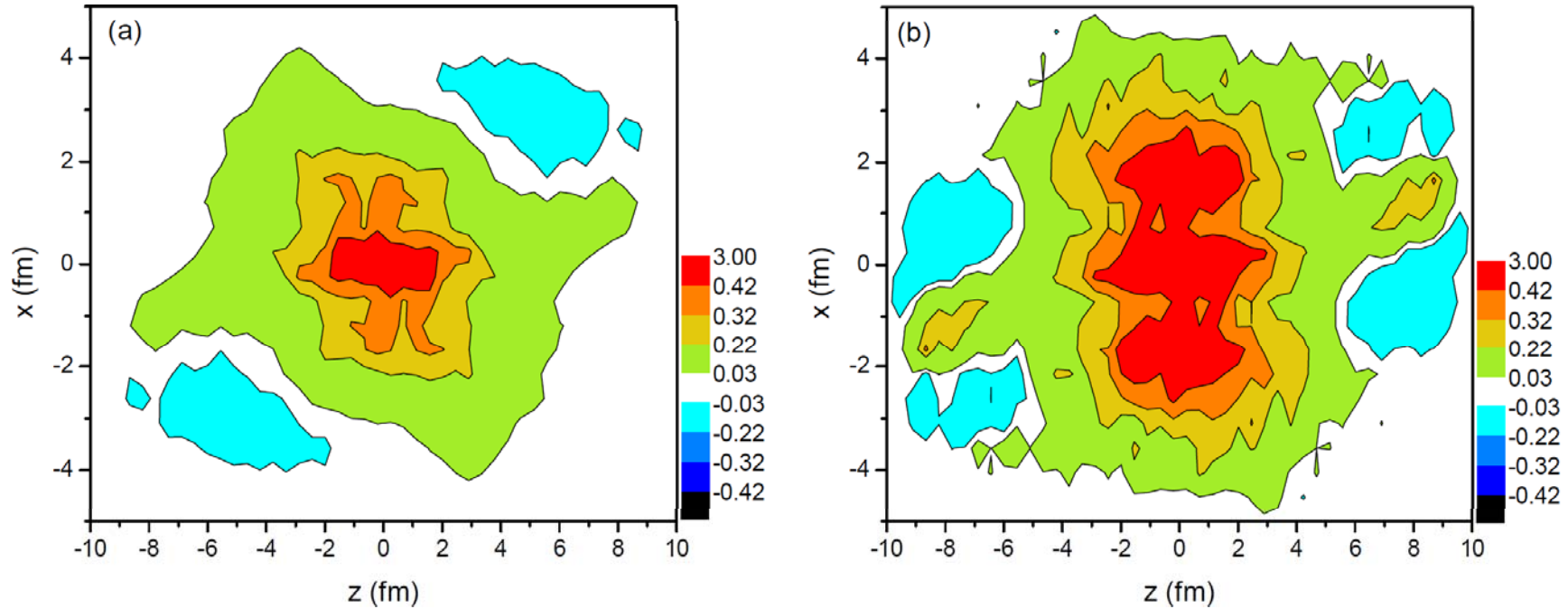


FIG. 5: The classical (left) and relativistic (right) weighted vorticity calculated for all [x-z] layers at t=3.56 fm/c. The collision energy is  $\sqrt{s_{NN}} = 2.76$  TeV and  $b = 0.7b_{max}$ , the cell size is  $dx = dy = dz = 0.4375 fm$ . The average vorticity in the reaction plane is 0.0538 / 0.10685 for the classical / relativistic weighted vorticity respectively.

Csernai, Magas, Wang, **PRC 87 (2013) 034906**

# Vorticity $\Rightarrow$ particle polarization

- T. Liang, X. N. Wang, PRL 94 (2005) 102301  
[Erratum-ibid. 96 (2006) 039901]

- B. Betz, M. Gyulassy, G. Torrieri, PRC 76 (2007)  
044901 (2007)

- J. H. Gao et al., PRC 77 (2008) 044902

- Becattini, Piccinini, Rizzo, PRC 77, 024906 (2008)

- Becattini, Csernai, Wang, arXiv:1304.4427,  
accepted to PRC

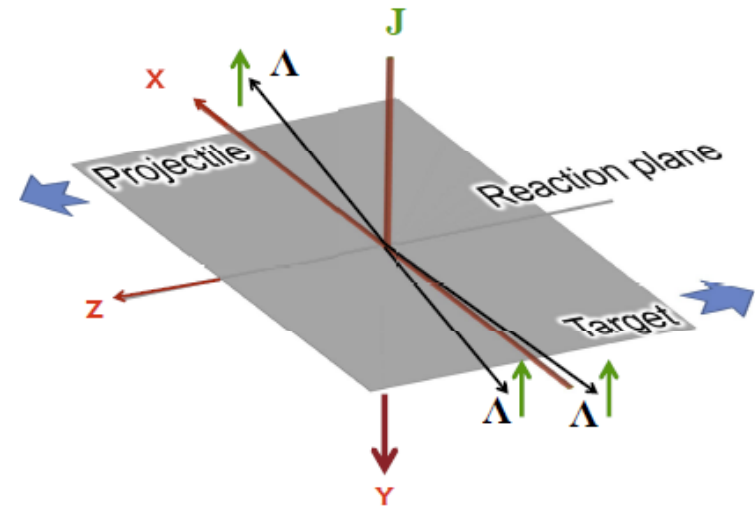
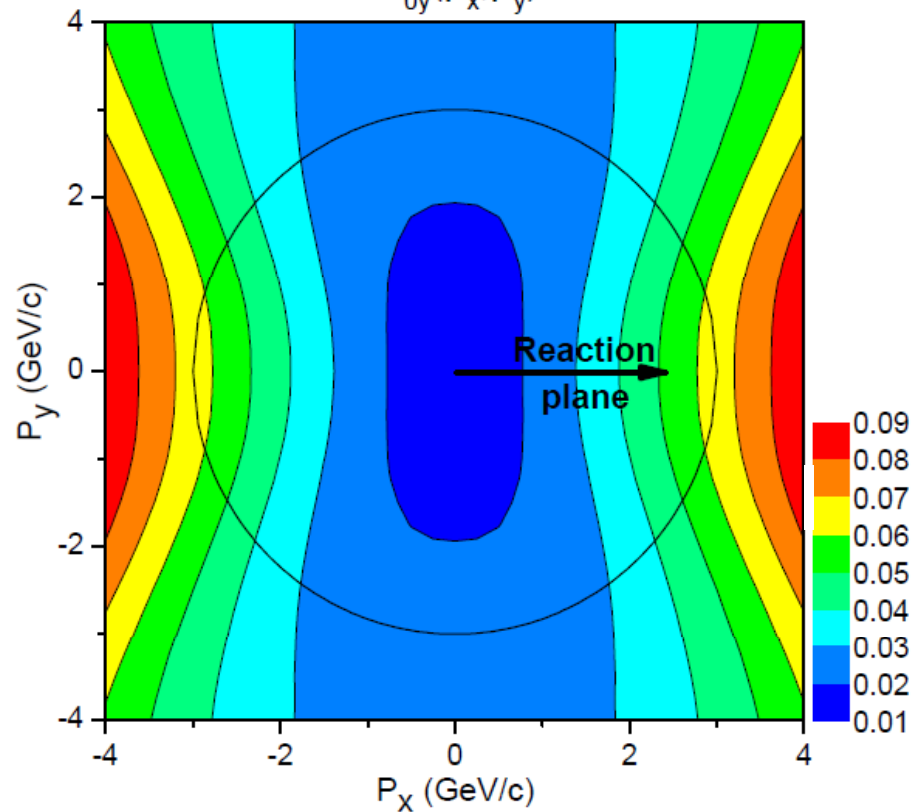
# Detecting rotation: Lambda polarization

$$\Pi(p) = \frac{\hbar \varepsilon}{8m} \frac{\int dV n_F (\nabla \times \beta)}{\int dV n_F}$$

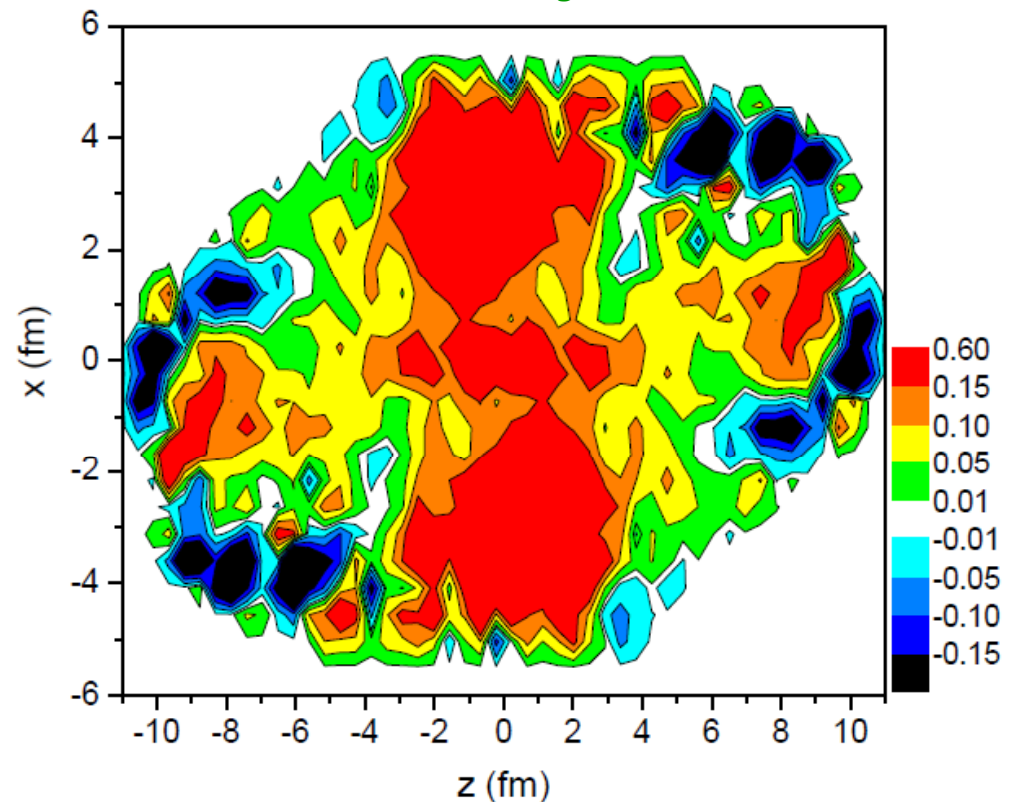
$$\beta^\mu(x) = (1/T(x)) u^\mu(x) \quad \leftarrow \text{from hydro}$$

$$\Pi_0(p) = \Pi(p) - \frac{\mathbf{p}}{\varepsilon(\varepsilon + m)} \Pi(p) \cdot \mathbf{p}$$

$$\Pi_{0y}(p_x, p_y)$$



Becattini, Csernai, Wang, arXiv:1304.4427



# Detecting initial rotation: Azimuthally sensitive HBT

UrQMD simulation

Pb+Pb

$E_{lab} = 8 AGeV$

Graef, Lisa, Bleicher,  
arXive 1302.3408

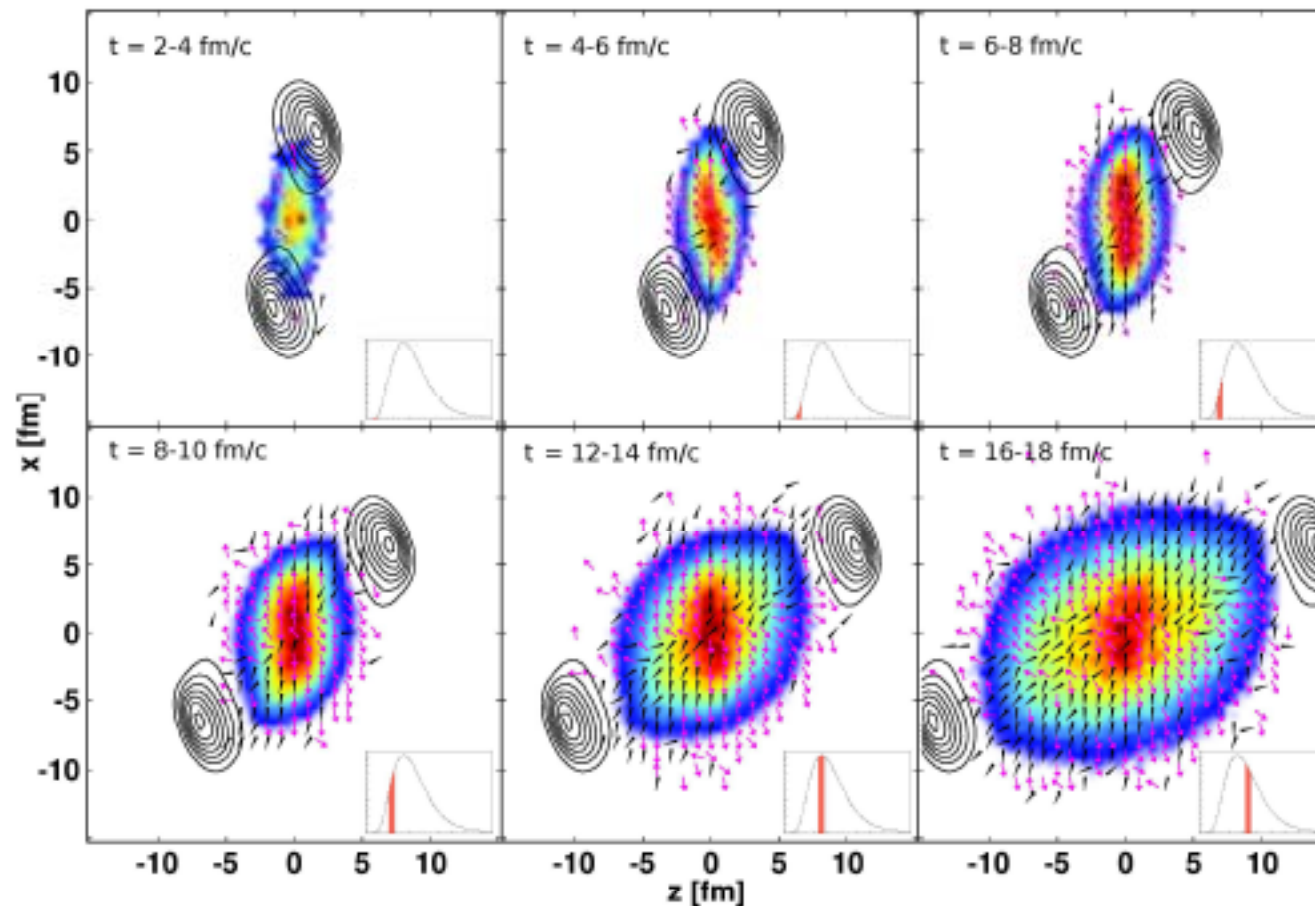


**Figure 3.** Shape of the freeze out region from pions frozen out at different times (colored surface). The contour lines depict the position of the spectators in each timestep. The vector field shows the direction of movement at each position and time. The black arrowheads contribute to the directed flow while the magenta arrows contribute to the antiflow. The inlay shows the freeze out luminosity of pions versus freeze out time. The shaded region in the inlay highlights the luminosity corresponding to the timestep in the overall picture.

# Detecting initial rotation: Differential HBT

L.P. Csernai, S. Velle , arXive 1305.0385

L.P. Csernai, S. Velle, D.J. Wang , arXive 1305.0396

$$\Delta C(k_{\pm}, q_{out}) \equiv C(k_{+}, q_{out}) - C(k_{-}, q_{out}) = \frac{4 \exp(-R^2 q^2) \epsilon \sinh\left(\frac{2u_z bk}{T_s}\right) (1-\epsilon^2) \left[1 - \cosh\left(\frac{u_z bq}{T_s}\right) \cos(aqd_x)\right]}{\left[(1+\epsilon^2) \cosh\left(\frac{2u_z bk}{T_s}\right) + (1-\epsilon^2)\right]^2 - 4\epsilon^2 \sinh^2\left(\frac{2u_z bk}{T_s}\right)}.$$

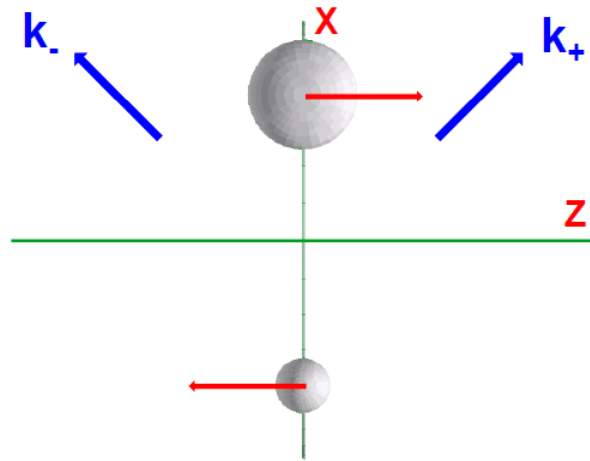


FIG. 14. (color online) Two moving sources in the reaction  $([x-z])$  plane, separated in the  $x$ -direction. The sources are moving in the directions indicated by the (red) arrows. The two "tilted" detector directions are indicated by the (blue) arrows labeled with  $k_+$  and  $k_-$ .

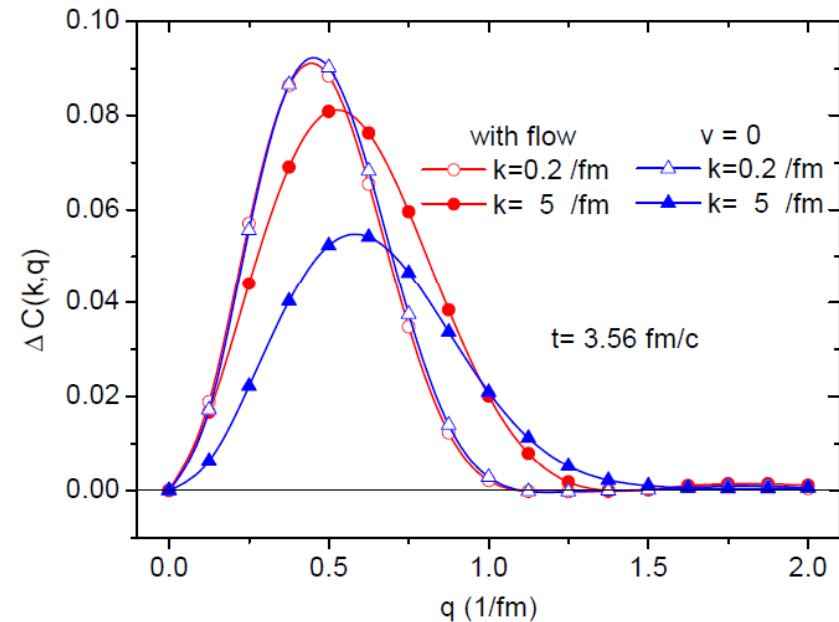


FIG. 3. (color online) The flow velocity dependence of the differential correlation function at the final time.



# Conclusions

Initial state with large initial angular momentum at LHC energies results in rotating "fireball"

The effect of such a rotation may be seen in:

- Directed flow,  $v_1$
- Elliptic flow,  $v_2$
- Particle polarization
- HBT

Back up

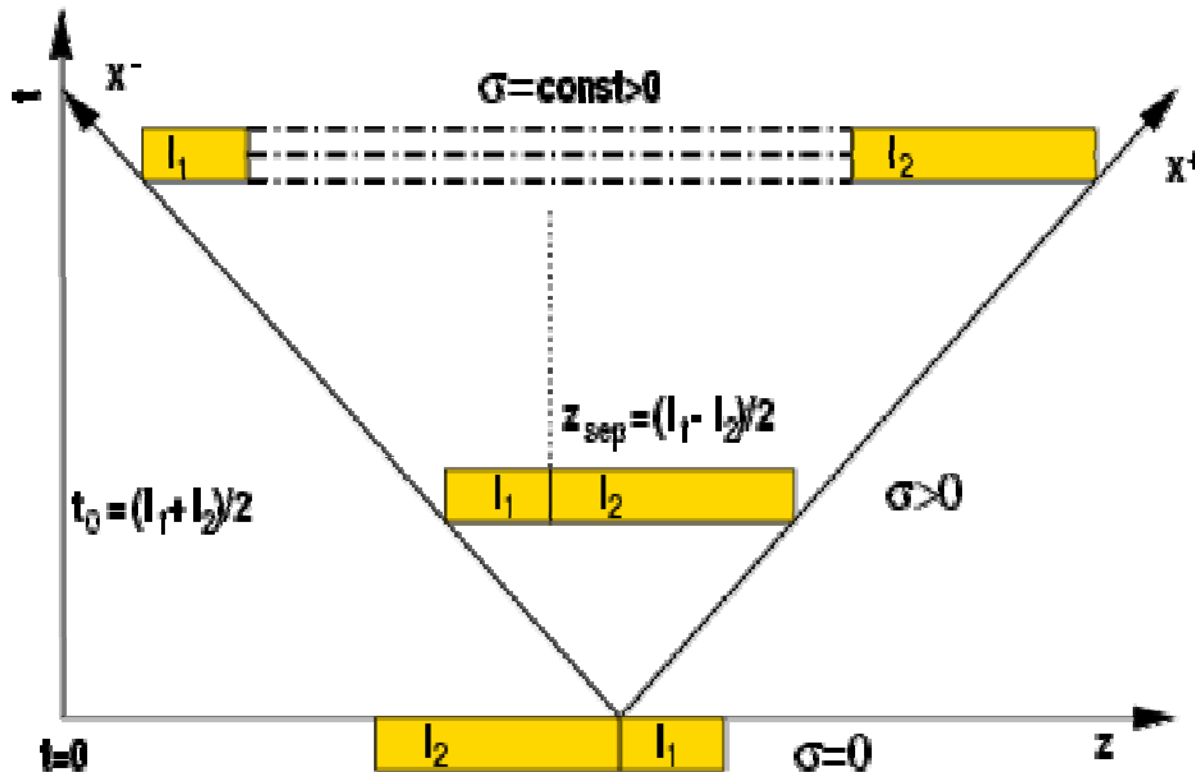
## Effective string rope model

Magas, Csernai, Strottman, PRC 64 (2001) 014901, NPA 712 (2002) 167

Transparency in the first moment

+ stretching chromoelectric field

+ energy-momentum conservation  $\rightarrow$   
deceleration of the colliding partons



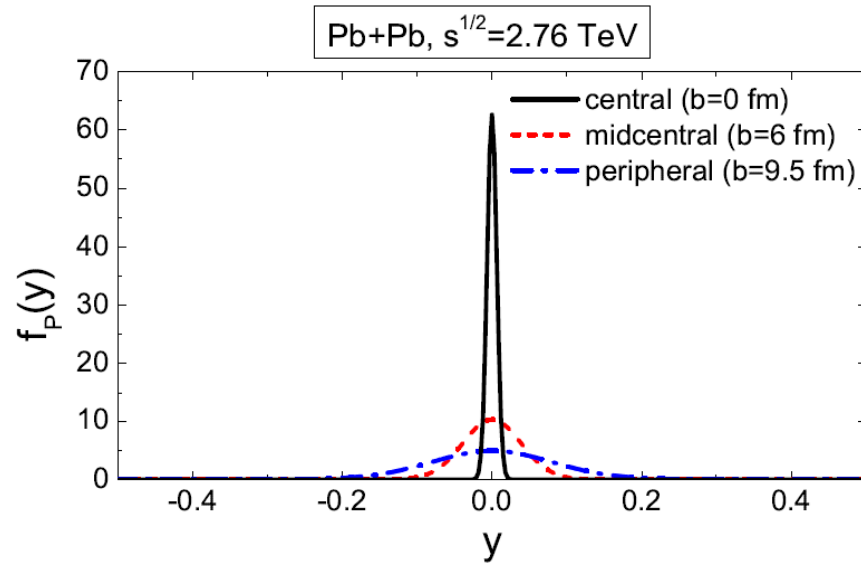
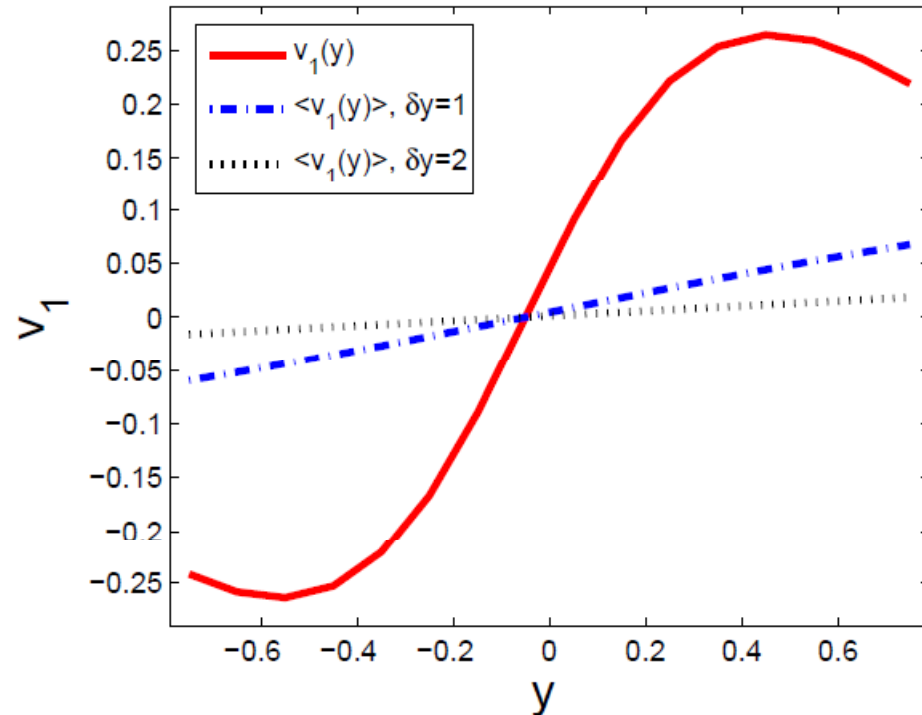


FIG. 5. Participant center-of-mass rapidity distribution for Pb+Pb collisions at  $\sqrt{s_{NN}} = 2.76$  TeV for three different centralities.

*$y_{CM}$  is fluctuating around “0”  
 with Gaussian distribution*

$$f(y_{CM}) = \frac{1}{\sqrt{2\pi\delta y^2}} e^{-y_{CM}^2 / \delta y^2}$$

Drastic effect:  
 no peaks ! ➡



Bleibel, Burau, Fuchs, PL B659, 520 (2008)

Similar results within  
quark-gluon string model  
with parton rearrangement

